`

SHEAR BEHAVIOUR OF ORDINARY STRENGTH RC SLENDER BEAMS

(Test on Beams with Minimal Shear Reinforcement and Average Longitudinal Reinforcement at Shear Span to Depth Ratio of 2.5)

By

Zakawat ALI

(NUST2012 60971 MSCEE15212F)

A Thesis submitted in partial fulfilment of

the requirement for the degree of

Master of Science

In

Structural Engineering

NUST Institute of Civil Engineering

National University of Science and Technology

Islamabad, Pakistan

(2016)

`

This is to certify that thesis entitled

SHEAR BEHAVIOUR OF ORDINARY STRENGHTH RC SLENDER BEAMS

(Test on Beams with Minimal Shear and Average Longitudinal Reinforcement at Shear span to Depth Ratio of 2.5)

Submitted by

Zakawat Ali

Has been accepted towards the partial fulfilment of the requirement for

Master of Science in Civil Engineering.

Brigadier (Retired) Dr. Khaliq-ur-Rashid Kayani	**Dr. Shaukat Ali Khan**
(Co-Supervisor)	**(Supervisor)**
NUST Institute of Civil Engineering,	**NUST Institute of Civil Engineering,**
NUST Islamabad	**NUST Islamabad**

`

National University of Sciences and Technology, H-12, Islamabad.

SHEAR BEHAVIOUR OF ORDINARY STRENGTH RC SLENDER BEAMS

(Test on Beams with Minimal Shear and Average Longitudinal Reinforcement at Shear Span to Depth Ratio of 2.5)

By

ZAKAWAT ALI

A Thesis

of

Master of Science

Submitted to the

NUST Institute of Civil Engineering

National University of Sciences and Technology

Islamabad, Pakistan

In partial fulfilment of the requirements

For the degree of

Master of Science in Civil Engineering

2016

`

Dedicated

To

My parents, teachers, family members

And

All Well wishers

`

ACKNOWLEDGEMENT

I am grateful to Almighty Allah whose blessing gave me the strength to complete this task. I am thankful to Dr. Shaukat Ali khan for his continuous guidance throughout this research project. I express my gratitude and sincere thanks to my co-supervisor Brigadier (Retired) Dr. Khaliq -ur- Rashid Kiyani for his advice and untiring guidance and supervision throughout the period of my research work. I am also thankful to the evaluation committee members for their guidance.

I am thankful to Mr. Ismail and other laboratory staff for their kind support for carrying out laboratory work. I also appreciate the supporting role of Mr. Akhtar Rasool, Muhammad Naeem and Muhammad Ashraf for providing assistance in testing of specimen.

I am also thankful to the administration of the NUST Institute of Civil Engineering and National Institute of Transportation for their help extended in the research work.

I appreciate full support provided to me by my parents and brother, this research work would not have been completed without their prayers and whole hearted encouragement.

`

ABSTRACT

Shear reinforcement in Reinforced concrete beams depends upon various parameters such as longitudinal steel ratio, aggregate type, strength of concrete, size of beam and types of loading. These factors are not fully incorporated in ACI code provision for design of minimum shear reinforcement. Zarari studied these factors on shear behavior of R.C beams analytically but experimentally have not been validated. To validate these factor, experimental work was undertaken on the shear behavior of ordinary strength reinforced concrete slender beams with moderate longitudinal reinforcement. Based on the experimental work, Modification to Zarari's equation is proposed on shear behavior of R.C beams.

The experimental program consisted of testing of eight simply supported R.C slender beams subjected to two concentrated loads with span to depth (a/d) ratio of 2.5.Test specimen were divided into four groups based on amount and spacing of minimum shear reinforcement in RC beams. Two specimens were prepared without shear reinforcement, two specimens were based on ACI code provisions, two specimens were prepared according to Zarari's (2003) equations, and two with modified equations presented in this study. Ultimate shear strengths obtained in this experimental program are compared to the analytical shear strengths calculated according to ACI code, Zarari equation and the Modified Zarari equation. Test results shows that, the proposed equation and Zarari equation gives better prediction of shear capacity of RC beams than ACI. Based on the test data, it was also found that minimum shear reinforcement should be such that it allows development of nominal flexural capacity in RC beams; accordingly a new expression for calculating minimum shear reinforcement is also proposed which incorporates all contributing factors.

`

Table of Contents

INTRODUCTION 1

1.1 General 1

1.2 Scope 2

1.3 Objectives 2

1.4 Methodology 2

LITERATURE REVIEW 3

2.1 Shear Strength of Concrete 3

2.2 Shear Transfer Mechanism 4

2.3 Shear Theories 6

2.3.1 Truss Model 6

2.3.2 Shear Theory 7

2.3.3 Modified Compression Field Theory (MCFT) 8

2.4 Parameters influencing Shear Strength 9

2.4.1 Shear Span to Depth Ratio (a/d) 9

2.4.2 Depth of Members or Size Effect 9

2.4.3 Axial Force 10

2.4.4 Longitudinal Reinforcement 11

2.4.5 Concrete Compressive Strength 11

2.4.6 Other Parameters 12

2.5 Failure Modes in Shear 12

2.5.1 Diagonal Failure 12

2.5.2 Flexural Failure 14

2.5.3 Anchorage Failure 14

2.5.4 Bearing Failure 15

2.6 Minimum Shear Reinforcement 15

2.6.1 Diagonal Crack Width and Minimum Shear Reinforcement 16

2.7 Zarari's Theory of Critical Shear Crack 17

2.7.1 Beams without Shear Reinforcement 17

2.7.2 Beams with Transverse Reinforcement 19

2.7.3 Minimum Shear Reinforcement 21

2.8 Modification in Zararis Theory 22

EXPERIMENTAL PROGRAM 24

3.1 GENERAL 24

3.2 Materials 24

3.2.1 Cement 24

3.2.2 Fine Aggregate 24

3.2.3 Coarse Aggregate 24

3.2.4 Reinforcing Steel 25

3.2.5 Super plasticizers 25

3.2.6 Water 25

3.2.7 Mix Design 25

3.3 Casting of Specimens 25

3.3.1 Test Specimens 25

3.3.2 Sample Preparation 26

3.4 Testing of Specimen 27

3.4.1 Test Setup 27

3.4.2 Test procedure 27

EXPERIMENTAL RESULTS 28

4.1 General 28

4.2 Deflection……28
4.3 Concrete Strength.....28
4.4 Behavior of Test Specimens.....28
4.4.1 Specimen N-1.....29
4.4.2 Specimen N-2.....29
4.4.3 Specimen A-1.....30
4.4.4 Specimen A-2.....30
4.4.5 Specimen Z-1.....31
4.4.6 Specimen Z-2.....31
4.4.7 Specimen MZ-1.....31
4.4.8 Specimen MZ-2.....32
4.5 Experimentation Summary.....33
TEST RESULT ANALYSIS, DISCUSSIONS AND CONCLUSIONS.....34
5.1 General…….....34
5.2 General behavior of beams.....34
5.3 Load Deflection Response:.....35
5.4 Modulus of Rapture of Concrete.....35
5.5 Shear strengths of Specimens.....36
5.6 Achieved Moment Capacity of Specimens and Minimum Shear Reinforcement.....37
5.7 Modifications to Zarari Equation.....38
5.8 Conclusions.....39
5.9 Recommendations.....40
Appendix-I.....41
Appendix-II.....49
Appendix -III.....68
References:……77

List of Tables

Table 3-1: CEMENT PROPERTIES 41

Table 3-2: PROPERTIES OF FINE AGGREGATE 41

Table 3-3: GRADATION OF FINE AGGREGATE 41

Table 3-4: PROPERTIES OF COARSE AGGREGATE 42

Table 3-5: COARSE AGGREGATE GRADATION 42

Table 3-6: HIGH RANGE WATER REDUCING AGENT. (TECHNICAL DATA) 42

Table 3-7: COMPRESSIVE STRENGTH RESULTS 43

Table 3-8: SPECIMEN DETAILS AND MATERIAL PROPERTIES 43

Table 4-1: Load Deflection Data of Beam N-1 50

Table 4-2: Load Deflection Data of Beam N-2 52

Table 4-3: Load Deflection Data of Beam A-1 54

Table 4-4: Load Deflection Data of Beam A-2 56

Table 4-5: Load Deflection Data of Beam Z-1 58

Table 4-6: Load Deflection Data of Beam Z-2 61

Table 4-7: Load Deflections Data of MZ-1 63

Table 4-8: Load deflection Data of Beam MZ-2 66

Table 5-1 Experimental and theoretical values of "μ" for Modulus of Rupture 69

Table 5-2: Shear Strengths of Specimens 69

Table 5-3: Experimental Values of γ for concrete shear strength 71

Table 5- 4: Achieved Flexural Capacity of Beams 74

`

List of Figures

Figure 2-1: Free body diagram of beam between two cracks (MacGregor) [3] 4

Figure 2-2: Internal forces in a cracked beam with stirrups (MacGregor) 5

Figure 2-3: Graphical representation of internal shears in beams 6

Figure 2-4: Comparison of large Scale Beam Tests by Shioya et al. with predictions from ACI Code and Modified Compression Field Theory (MCFT). 10

Figure 2-5: Diagonal tension failure 13

Figure 2-6: Shear tension failure 13

Figure 2-7: Shear compression failure 14

Figure 2-8: Flexural failure 14

Figure 2-9: Anchorage failure 15

Figure 2-10: Bearing failure 15

Figure 2-11: Cracking pattern of slender beams 18

Figure 2-12: Stress distribution along line of splitting (+: tension, -: compression) 19

Figure 2-13: Distribution of forces in beam (based on Zararis theory). 20

Figure 2-14: Forces acting in the region of horizontal splitting along the longitudinal reinforcement of beam (a) without stirrups, (b) with stirrups at spacing, s= lt and (c) with s< lt 21

Figure 3-1: Stress-Strain Relationship of Longitudinal bar 44

Figure 3-2: Gradation of Fine Aggregates 44

Figure 3-3: Gradation of Coarse Aggregates 45

Figure 3-4: Specimen dimensions and details 46

Figure 3-5: Specimens transporting to lab with the help of crane 47

Figure 3-6: Test Setup 48

Figure 3-7: Beam Form Work 48

Figure 4-1: Structural Load Analysis and Automation System 49

`

Figure 4-2: Load Deflection Plot N-1 51

Figure 4-3: Cracking Pattern of N-1 51

Figure 4-4: Load Deflection Plot N-2 53

Figure 4-5: Cracking Pattern of Beam N-2 53

Figure 4-6: Load Deflection Plot A-1 55

Figure 4-7: Cracking Pattern A-1 55

Figure 4-8: Load Deflection Plot A-2 57

Figure 4-9: Cracking Patterns A-2 57

Figure 4-10: Load Deflection Plot Z-1 59

Figure 4-11: Cracking Patterns Z-1 60

Figure 4-12: Load Deflection Pot Z-2 62

Figure 4-13: Cracking Pattern Z-2 63

Figure 4-14 : Load Deflection Plot of Beam MZ-1 64

Figure 4-15 : Cracking Pattern MZ-1 65

Figure 4-16 : Load Deflection Plot MZ-2 67

Figure 4-17 : Cracking Pattern MZ-2 67

Figure 5-1 : Average Load Deflection Response of Beams 68

`

Figure 5-2 : Transverse Steel Ratio Vs Ultimate Shear Strengths Comparison of Specimens 70

Figure 5-3: Variation in Experimental Shear Strength From ACI Theoretically calculated Shear Strength..... 70

Figure 5-4 : Variation in Concrete Contribution from ACI Predicted Strengths..... 71

Figure 5-5 : Experimental Trend of γ for concrete shear Strength..... 72

Figure 5-6 : Shear Strength Variation from Zarari's Equation 73

Figure 5-7 : Shear Strength Variation from Modified Zarari Equation. 73

Figure 5-8 : Transverse Steel Ration vs Achieved Moment Capacity..... 74

Figure 5-9 : Transverse Steel ratio Vs Achieved shear Strength..... 75

`

LIST OF ABBREVIATIONS/NOTATIONS

f'c	Compressive concrete strength
fy	Yield strength of longitudinal reinforcement
fyv	Yield strength of shear reinforcement
M	Moment
Mn	Nominal moment strength according to ACI Code
V	Shear force
Vd	Dowel force due to longitudinal reinforcement
Vcr	Critical shear force in beam without stirrups
Vccr	Critical shear force in concrete
Vdcr	Critical shear force in longitudinal steel
Δ Vd	Increase in dowel force due to stirrups
Ld	Development length
lt	Splitting length
α	Factor for development length
s	Stirrups spacing
ρ	Longitudinal reinforcement ratio
b	Beam width
d	Effective depth of beam
h	Overall height of beam
Vc	Shear strength provided by concrete
Vs	Shear strength provided by concrete
A	Shear span
Vn	Nominal shear strength
As	Area of longitudinal steel
w/c	Water cement ratio
mm	Millimeter
in	Inch
psi	Pounds per square inch
ksi	Kilo pounds per square inch
γ	Factor for predicting shear force provided by concrete
μ	Factor for calculating modulus of rupture

`

INTRODUCTION

1.1 General

Reinforced concrete is widely used construction material for rapid urbanization and industrialization .Over the year's extensive research has been carried out to understand the failure mechanism and to improve the quality of reinforced concrete. The use of reinforced concrete has increased due to its various fore deals like high modulus of elasticity, chemical resistance, frieze thaw resistance, low creep, shrinkage and permeability.

Reinforced concrete has various modes of failure but unlike other modes of failure shear failure are less predictable .Shear failure is a prominent mode of failure with little or no warning .Shear failure mechanism is complex and based upon various parameters such as

I. longitudinal steel ratio
II. Aggregate type
III. Strength of concrete
IV. Typed of loading
V. Support condition
VI. Web width
VII. Crack control steel
VIII. Size of beam

On the basis of these parameters extensive research has been carried out to predict the actual behavior of shear failure and from time to time changes has been made in international codes based on research work .Parameters affecting shear strength of beam has led to large no of shear design methods. Various codes are develop to predict actual behavior of shear strength but when these codes are compared with experimental results these codes are either conservative or sometimes it undermines the effect of various parameters .A number of new theories are emerging and international codes are adopting these theories but there is no appropriate relationship to predict with accuracy the shear strength of slender beams incorporating the contributing parameters affecting the shear strength of beams.

`

1.2 Scope

The purpose of this research work is to study the shear behavior of reinforced concrete slender beams incorporating the contributing parameters affecting the shear strength of beams .The research is to determine the factors influencing the shear capacity of R.C slender beams that are not part of the present ACI code equations for minimum web reinforcement .This study also includes the theory presented by Prodromos Zarari which postulate that shear collapse is due to the formation of critical shear crack, made of two branches. For this purpose experimental program is conducted to attain the objective of research project.

Full scale sample of ordinary strength reinforced concrete slender beams reinforced according to ACI as well as Zarari theory will be tested at shear span to depth ratio of 2.5.

1.3 Objective

- To find out the correctness of rife expressions for predicting the ultimate shear capacity of reinforced concrete beam.
- To establish a min shear reinforcement requirement of reinforced concrete beam in presence of longitudinal reinforcement ratio and shear span to depth ratio.
- To ascertain effect of longitudinal reinforcement ratio and shear span to depth ratio in the shear strength provided by concrete in reinforced concrete slender beams.

1.4 Methodology

The literature review focusing on available research on shear behavior of RC beams has been carried out. The experimental study based on the review has been devised. Eight full scale rectangular beams having moderate longitudinal reinforcement were cast and tested at shear span to depth ratio of 2.5

These samples are described as under:-

- Beams without shear reinforcement – 2
- Beams with ACI minimum shear reinforcement – 2
- Beams with minimum amount of shear reinforcement as specified by P.D. Zarari – 2
- Beams with minimum amount of shear reinforcement estimated after incorporating changes in Zarari equation – 2

LITERATURE REVIEW

2.1 Shear Strength of Concrete

In a 1935 Engineering News Record review article for structural design engineers, Professor Hardy Cross quoted with approval of the paradoxical statement of the Cambridge astrophysicist Sir Arthur Eddington that "No experiment is worthy of credence unless supported by an adequate theory. (Collins, Bentz, Sherwood and Xie, 2007) [6]

In concrete member when the moment is not constant over its length, shear forces are required to be considered. Almost all flexural members are subjected to shear stresses which may result in diagonal cracks. These diagonal cracks can cause premature failure of the member, which is expected to be a brittle and unstable mechanism. To guard against such phenomenon, appropriate amounts of properly detailed transverse and longitudinal reinforcement should be provided. For determining flexural strength of concrete beams, theory based on Hooke's Law is used which implies that stress is proportional to strain and plane sections remain plane before and after bending. For finding the shear strength of concrete beams, we have following two cases:-

Beams with Shear Reinforcement: When beams are equipped with shear reinforcement or stirrups, their shear resistance can be ascertained using the truss analogy developed by Ritter and Morsch. The upper bound solution is used to minimize the strengthening effect of the stirrups (Braestrup, 2009) [7].

Beams not having Shear Reinforcement: In the absence of shear reinforcement, only shear transfer mechanism provides the requisite shear resistance. This primarily is the point where codes of practice lack a theory and use totally empirical procedures. (Collins, Bentz, Sherwood and Xie, 2007) [6]

`

2.2 Shear Transfer Mechanism

In reinforced concrete beams, shear is transferred by two load transfer mechanisms: beam action and arch action. The contribution of beam action and arch action depends on shear span to depth ratio (a/d ratio). Normally, beam action is the governing load transfer mechanism in slender beams (a/d ratio greater than 2.5) whereas arch action is dominant mechanism in deep beams (a/d ratio less than 2.5). The two shear transfer mechanisms can be expressed mathematically by considering a free body diagram of the portion of a reinforced concrete beam between two cracks as shown in Figure 2.1. Shear force (V) is related to the tensile force in the bar (T) as under:

$$V = \frac{d}{dx}(TJd)$$

$$\Rightarrow V = \frac{d(T)}{dx} + \frac{d(Jd)}{dx}$$

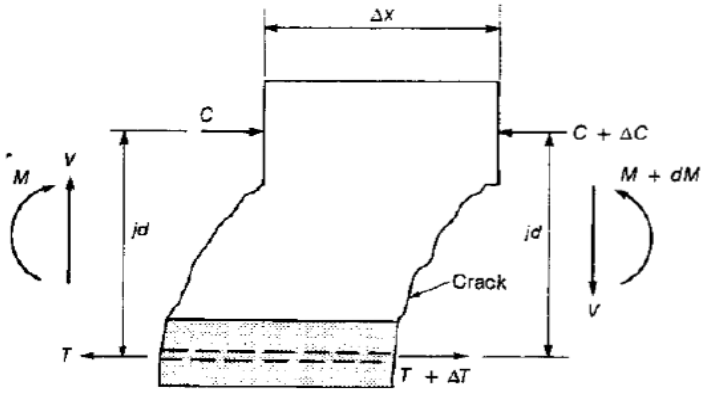

Figure 2-1 Free body diagram of beam between two cracks *(MacGregor)* [3]

If the lever arm (*jd*) remains constant as assumed in elastic beam theory, the shear force is transferred in beam action (V_b) as follows:

$$\frac{d(Jd)}{dx} = 0 \quad and \quad V = V_b = \frac{d(T)}{dx}$$

Where $V = d(T) / dx$ is the shear flow across any horizontal plane between the reinforcement and the compression zone. For beam action to exist shear flow must be present. On the other

`

hand if the shear flow, *d(T) / dx* equals zero, then the shear force is transferred to arch action (V_a) as follows:

$$V = V_a = \frac{d(Jd)}{dx}$$

This happens when the reinforcing steel is un bonded and the shear flow cannot be transmitted, or when an inclined crack extend from the load point to the support preventing the transfer of shear flow. In such cases, shear is transferred by arch action instead of beam action (MacGregor) [3].

According to experimental and analytical research, it has been revealed that the primary mechanisms of shear resistance include force provided by concrete in compression zone, aggregate interlock and the dowel action across the longitudinal steel bars. Any shear force, surplus to above three mechanisms, is resisted by steel stirrups which are generally vertically placed and suitably anchored in compression zone to avoid slipping. In a cracked reinforced concrete beam with shear reinforcement, the shear is carried by the vertical component of shear force in compression zone concrete (V_{cy}), Vertical component of aggregate interlock force at the cracked surface (V_{ay}), the dowel action of longitudinal reinforcement (V_d) and the force in the vertical stirrups (V_s). Internal distribution of the forces is shown in Figure 2.2.

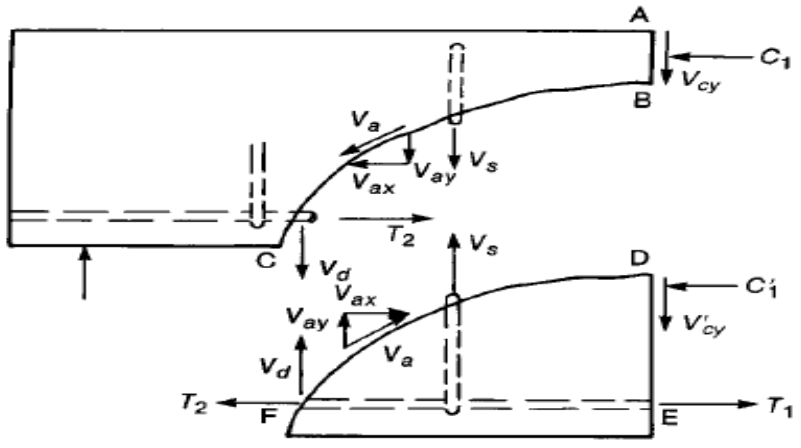

Figure 2-2Internal forces in a cracked beam with stirrups (MacGregor)

`

Distribution of internal shear forces in a beam with web reinforcement, at various stages of loading or applied shear, can be graphically represented as in Figure 2.3

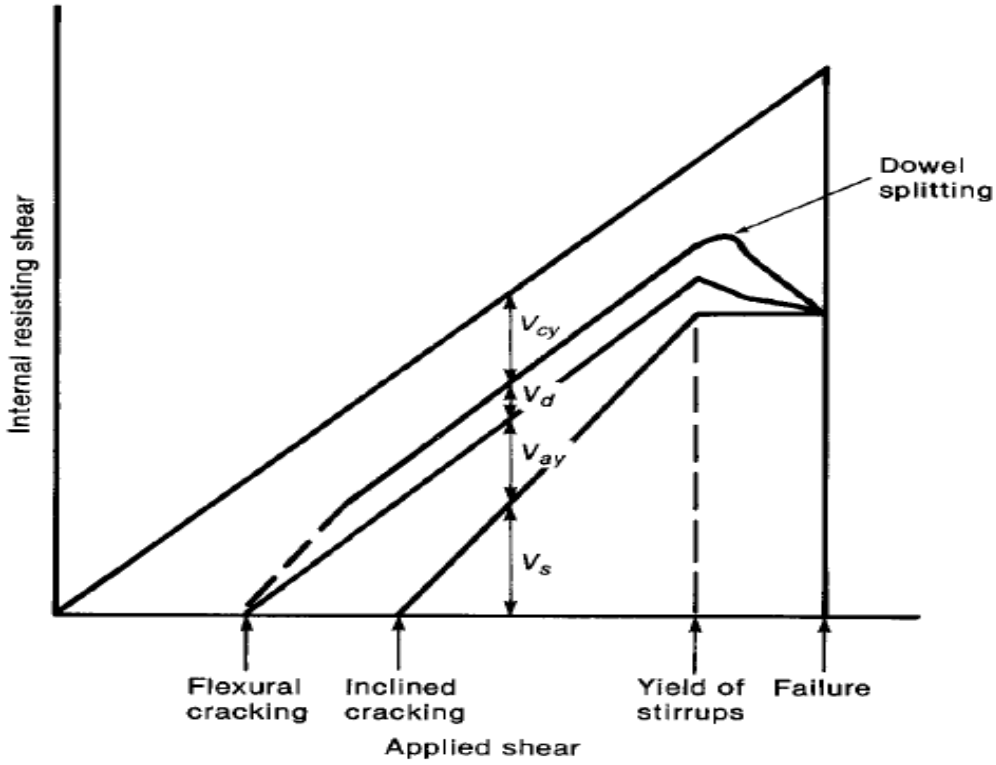

Figure 2-3 Graphical representation of internal shears in beams

2.3 Shear Theories

2.3.1 Truss Model

Mechanical mathematical models can be used to express the behavior of beams failing in shear. Most suited model for beams with shear reinforcement is the truss model. The Swiss engineer Ritter[2] and the German engineer Morsch[1], in their independent works, proposed the truss analogy for the design of reinforced concrete beams for shear (1899 to 1902). It provided an excellent conceptual model to depict the forces existing in a cracked concrete beam.

Compressive and tensile forces, C and T respectively, are developed in beams with inclined cracks, in its top and bottom portions. Other forces acting in these beams are tension in the vertical stirrups and inclined compressive forces in the concrete "diagonals" between the inclined cracks as shown in (Figure 2.1-Appendix I). This highly indeterminate system of forces is replaced by an analogous truss.

`

To derive the analogous truss, several simplifications and assumptions are required (Figure 2.2-Appendix I). The truss has been formed by combining all the stirrups cut by section A-A into one vertical member b-c and all the diagonal concrete members cut by the section B-B into one diagonal member b-d. This diagonal member is stressed in compression to resist the shear on section B-B. The compression chord along the top of the truss is actually a force in the concrete but is shown as a truss member. The compressive members in the truss are shown with broken lines and the tensile members with solid lines (Mc Greggor) [3].

2.3.2 Shear Theory

The shear stresses, *v*, on elements of a beam section can be calculated by traditional theory for homogenous, elastic, un cracked beams as:-

$$v = \frac{VQ}{Ib} \tag{2.1}$$

Where,

V = Shear force on a cross section

Q = First moment about the neutral axis

I = Second moment of area of cross section

b = Width of member where stresses are being calculated.

It should be noticed that equal shearing stresses exist on both the horizontal and vertical planes through an element (Figure 2.3-Appendix I). The horizontal shear stresses are of importance in the design of construction joints, web-to-flange joints, or regions adjacent to the holes in beams. For an un-cracked rectangular beam, Equation 2.1 gives the distribution of shear stresses.

However, this equation is not applicable to reinforced concrete beams for the following reasons:

- Reinforced concrete comprises two materials having significantly different strength and stiffness and is thus heterogeneous.

`

- Concrete is subjected to creep therefore, it is not elastic.
- Cross sections of the beams may be cracked or un cracked. Since the extent of cracking at a specified location along the length of the beam is unpredictable, the actual cross sectional properties on which to base computations of moment of inertia and moment of area etc. cannot be accurately determined.
- Because of cracking, the effective cross section of reinforced concrete members is variable along their length.

Because of the above-mentioned reasons, correct evaluation of shear stress intensity in a reinforced beam is not possible. The ACI 2011 has therefore adopted a simple procedure for establishing the order of magnitude of the average shear stress on a cross section. The shear stress is computed by dividing the shear force by $b_w d$, the effective area of concrete.

$$v = \frac{V}{b_w d} \tag{2.2}$$

Where, v = Shear stress at a section

V = Shear force at section

b_w = Beam width

d = Distance between top surface and centroid of bottom steel

2.3.3 Modified Compression Field Theory (MCFT)

It has been shown by researchers that, the inclination of the concrete compression is not necessarily 45 degrees, and that a more realistic basis for shear design is provided by equations based on variable angle truss. Moreover, tests of reinforced concrete panels subjected to pure shear improved the understanding of the stress-stain characteristics of diagonally cracked concrete. An analytical model called the modified compression field theory was developed by utilizing the concrete stress-stain relationship. This model has proved to be capable of accurately predicting the response of reinforced concrete subjected to shear. Load transmission in cracked reinforced concrete comprises relatively complex mechanisms involving opening or closing of pre-existing cracks, formation of new cracks, interface shear transfer at rough crack surfaces, and significant variation of stresses in reinforcing bars due to bond, with the highest

`

steel stresses occurring at crack locations. The modified compression field model attempts to capture the essential features of this behavior without considering all of the details. The crack pattern is idealized as a series of parallel cracks all occurring at angle θ to the longitudinal direction. The shear stress that can be transmitted across the crack is a function of the crack width *w*, aggregate size *a*, and is given as (Mitchell and Collins) [8].

$$V_{ci} = \frac{2.16\sqrt{f_c'}}{0.3 + \frac{24w}{a + 0.63}} \qquad (2.3)$$

2.4 Parameters influencing Shear Strength

2.4.1 Shear Span to Depth Ratio (a/d)

The average shear stress at failure is progressively larger for deeper members (a/d ratio below 2.5) rather than in slender beams. This is because of the fact that, in deep members, shear can be easily transmitted directly to the support by means of compression struts. If a direct compression strut will be formed, the conditions on the supports become important. When a member is loaded on the top face and supported on the bottom face, it is more likely to form such a strut (Adebar 1994) [9]. The strut-and-tie model approach should be used for designing the members in which a direct compression strut is expected to form, rather than a sectional design procedure. Furthermore, the *a/d* ratio is used to describe a shear failure mechanism of simply supported, plain concrete beams, loaded with point loads. That was the result that Leonhardt and Walter (1966) [10] observed after testing beams cast with normal strength concrete.

2.4.2 Depth of Members or Size Effect

Many tests on the shear behavior of relatively small beams have been carried out in the last decades. It was revealed that the results of these tests cannot be directly applied to full size beams. Kani (1967) [11] showed that for members without shear reinforcement, there is a very

`

significant size effect on the shear strength of these members. The shear strength of these members tends to decrease with the increase in effective depth. This fact was reaffirmed by Shioya. Figure 2.4 explains the effect of size of the member on shear strength. Primary reason for this size effect is believed to be increased widths of diagonal cracks.

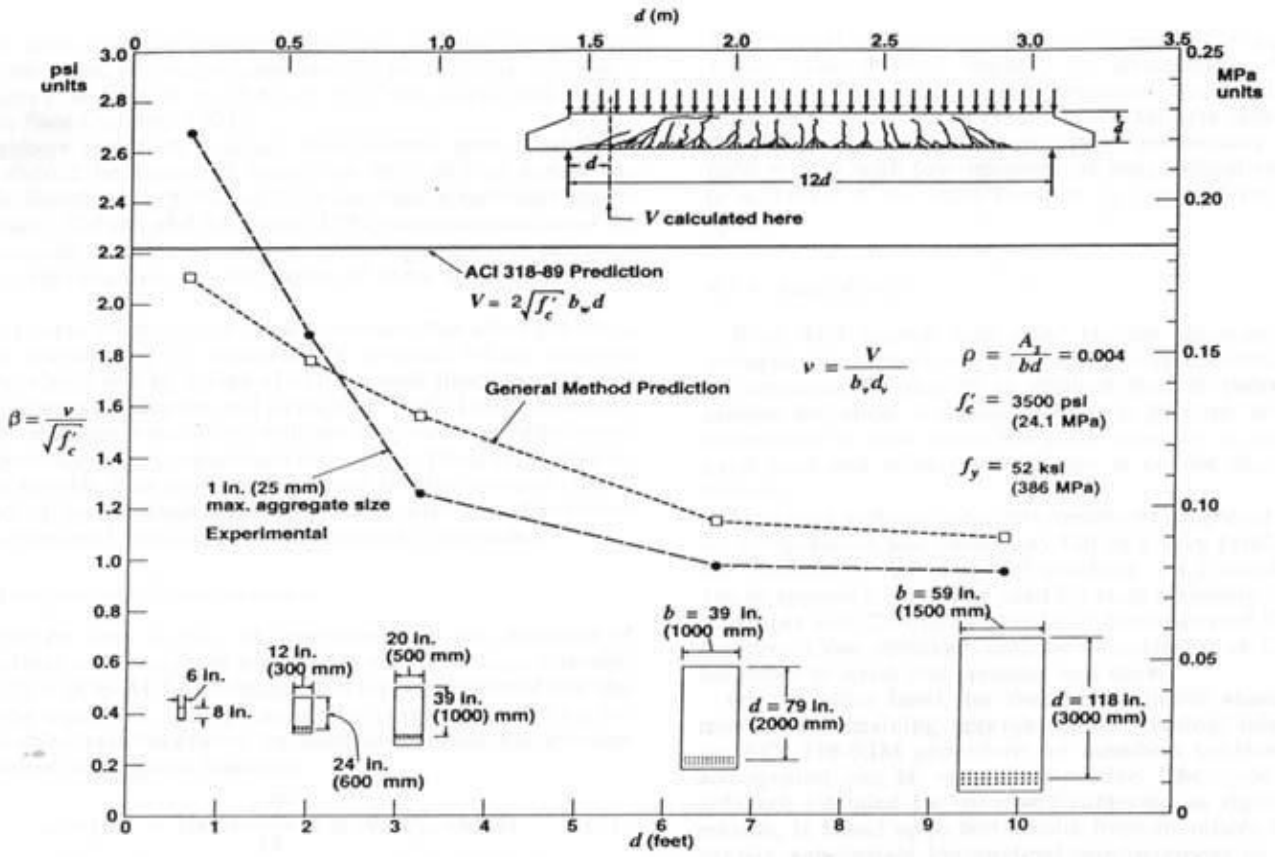

Figure 2- 4 Comparison of large Scale Beam Tests by Shioya et al. with predictions from ACI Code and Modified Compression Field Theory (MCFT)

2.4.3 Axial Force

Shear strength is also dependent on axial force particularly for members without transverse reinforcement. The shear strength of members deceases with an axial tension and increases with an axial compression which may be in the form of applied load or pre-stressing. However, extent of effect of axial force on shear capacity and ductility of the member is still a point of debate in the research community. Very brittle failure is expected in members subjected to axial compression and shear even at the time of initial diagonal cracking. Collins and Gupta (1993) [12] had shown that the ACI Code approach may not be conservative for members subjected to shear and axial compression. Axial load affects the magnitude of shear at

`

the onset of flexural cracking, which was found by Mattock (1969) [13]. The diagonal cracks in members appear to be less than 45° when axial compression is present. Therefore use of the design approach for web reinforcement based on the truss analogy with 45° struts is conservative.

2.4.4 Longitudinal Reinforcement

Kani investigated the influence of longitudinal steel ratio on shear behavior of members. It is important to note that, although, a higher amount of steel improves the shear response of a member, it definitely makes the failure more brittle and sudden. Kim and Lee (2008) [14] have conducted tests on 26 reinforced concrete beams with minimum shear reinforcement. In their study, reserve strength has been defined as the ratio between the ultimate shear capacity of the beams with the minimum shear reinforcement and that of the beams without shear reinforcement. Likewise, reserve deflection is defined as the ratio between the deflection corresponding to the ultimate load of beams with minimum shear reinforcement and the deflection of beams without shear reinforcement. They had concluded that the amount of minimum shear reinforcement needs to increase / decrease as ρ_l decreases / increases to achieve uniform reserve strength and deflection. It is worth mentioning that, from structural design point of view, a good reinforcement ratio ρ should be balanced after taking into account both shear and flexure mechanisms.

2.4.5 Concrete Compressive Strength

As a result of eleven test series conducted on rectangular reinforced concrete beams by Kani, he concluded that the shear strength does not depend on compressive strength of concrete. However, it should be noticed that Kani tested beams with compressive strength ranging from 18 to 36 MPa. Later studies revealed that the effect of compressive strength is quite noticeable in high strength concretes. Now, it is strongly believed that concrete compressive strength fc' has a significant effect on the ultimate shear strength of concrete members, since shear forces are resisted by concrete and transverse reinforcement. It is not theoretically possible to assess the individual components which describe the concrete contribution to shear. Some researchers (Taylor) [15] have attempted to determine experimentally each of these components for Normal strength concrete (NSC). They have

`

shown that in case of NSC, compressive strength is normally less than the crushing strength of the aggregates. Therefore, the crack skirts across the aggregates. This means that, due to the uneven and jagged surface of the crack, the aggregate interlock component of shear resistance is enhanced. Some researchers and designers are doubting that High strength concrete (HSC) may not be strong in shear because of the aggregate interlock mechanism, which may be absent in HSC. Due to the smaller difference in the strength of aggregates and the concrete matrix, the crack surfaces are smoother compared to NSC (Konig 1993) [16], which means that the aggregate interlock between the fracture surfaces will be reduced. Some tests done by Pendyala and Mendis (2000) [17] showed that the shear strength of concrete beams does not increase significantly in the range of 30 to 70 MPa. In a study by Reineck et al [18], beams made with 100 MPa concrete failed at about the same shear stress as beams made from 35 MPa concrete.

2.4.6 Other Parameters

Besides the parameters described above, other parameters not considered so crucial by the researchers but can affect the shear resistance of a member are as under:-

- Load conditions
- Cross section shape
- Distribution of longitudinal reinforcement

2.5 Failure Modes in Shear

2.5.1 Diagonal Failure

Several structural concrete members like slabs, columns, beams and corbels etc have also been reported to have failed due to shear distress or diagonal failure. Mechanism of transfer of shear in all members is believed to be the same, however, cracking pattern may vary. Diagonal failure is caused due to a combination of shear force and the bending moment (Ziara, 1993) [19].

2.5.1.1 Diagonal Tension Failure

The diagonal crack initiates from the last flexural crack formed. In case of slender beams (a/d between 2.5 and 6), failure occurs within the shear span (a). The crack propagates through the beam and reaches the compression zone and at critical loading, it is likely to fail as

`

a result of splitting of concrete there which is expected to happen suddenly in a brittle manner as shown in Figure 2.5 (Ziara, 1993) [19].

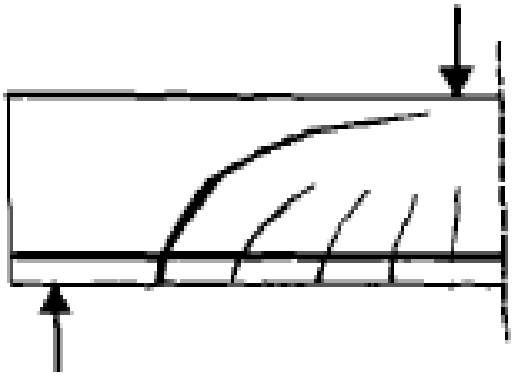

Figure 2- 5Diagonal tension failure

2.5.1.2 Shear Tension Failure

The difference between diagonal tension failure and this type is that it applies to short beams. In this case too, the shear crack propagates through the beam but is not likely to cause the failure at its own. Loss of bond between concrete and longitudinal steel can also cause failure due to splitting cracks developing in this region (Figure 2.6). On reaching a critical loading point, beam fails as a result of splitting of the compression concrete (Ziara, 1993) [19].

Figure 2- 6 Shear tension failure

2.5.1.3 Shear Compression Failure

Contrary to shear tension failure, if splitting cracks do not appear and the failure is caused merely due to diagonal shear crack propagating through the beam, it is termed as a shear

`

compression failure (Figure 2.7). This failure mode mainly applies to deep beams. In short beams, due to presence of arch action, the ultimate load causing failure can be much larger.

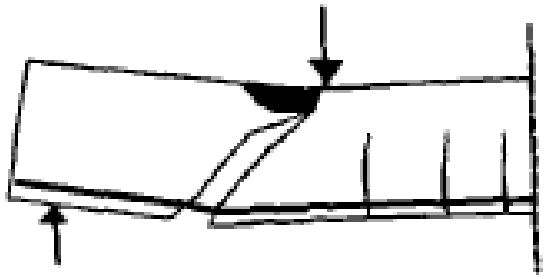

Figure 2- 7 Shear compression failure

2.5.2 Flexural Failure

Moment is basically responsible for initiation and propagation of flexural cracks which occur in slender beams. AT the location where moment in the beam is maximum, appearance of cracks is more likely (Figure 2.8). When the shear stress in the concrete reaches its tensile strength, cracks develop. Flexural cracks are almost vertical and cause failure to the beam either due to excessive yielding of longitudinal reinforcement in case of under reinforced beams, which may cause failure of concrete in tensile zone or due to crushing of concrete in compression zone before the longitudinal reinforcement yields (Ziara, 1993) [19].

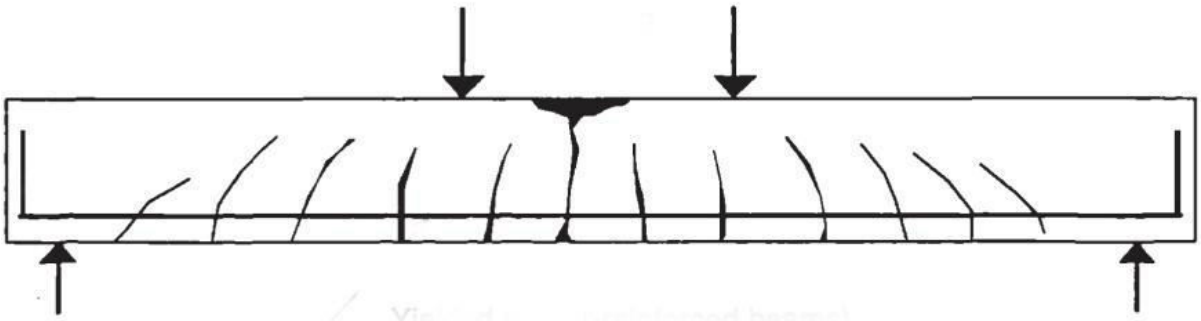

Figure 2- 8 Flexural failure

2.5.3 Anchorage Failure

`

Anchorage failure may be described as a slip or loss of bond of the longitudinal reinforcement (Figure 2.9). It can be linked to dowel action where the aggregates interlocking resistance around the bar has failed resulting in splitting of the concrete.

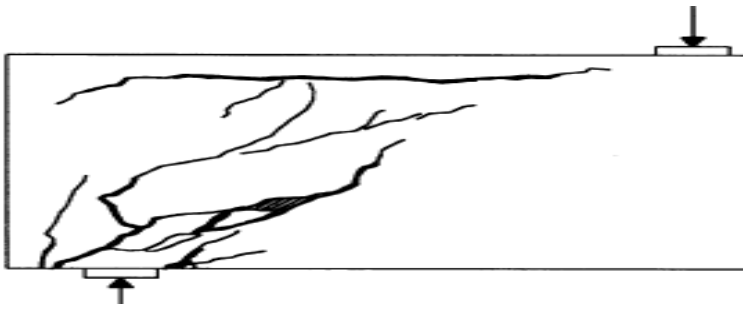

Figure 2-9 Anchorage failure

2.5.4 Bearing Failure

When bearing stresses exceed the bearing capacity of the concrete, it results in failure of the support. If size of bearing plate is too small, it will result in failure if concrete at the support as in Figure 2.10.

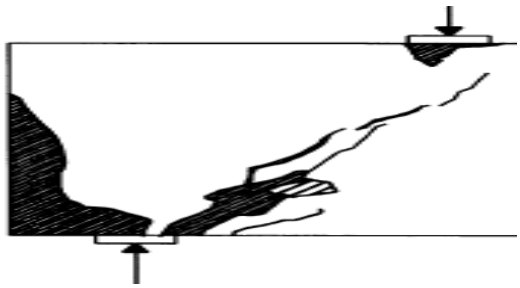

Figure 2-10 Bearing failure

2.6 Minimum Shear Reinforcement

To avoid abrupt shear failure, ACI 318 – 11 specifies that minimum amount of shear reinforcement must be there in reinforced concrete beams. This minimum amount of transverse steel is intended to restrain the growth of diagonal cracks to avoid abrupt shear failure. Basing on previous experimental data for beams of normal and high strength concrete, ACI equation for minimum shear reinforcement has been developed. This equation is believed to have little consideration for the effects of longitudinal reinforcement and shear span to depth ratio (Lee & Kim 2008)[14].

`

When minimum amount of shear reinforcement is provided in the beams, it holds the two cracked faces together, thus preventing the loss of shear transfer by aggregate interlock. Where required, the minimum shear reinforcement shall be computed by the equations (ACI Section 11.4.6.3) reproduced below. Equation 2.4 is new in the code and was introduced in ACI 318-05 to account for the influence of compressive strength of concrete.

$$A_{v,\min} = 0.75\sqrt{f'_c}\,\frac{b_w s}{f_{yt}} \qquad (2.4)$$

But not less than

$$A_{v,\min} = 50\,\frac{b_w s}{f_{yt}} \qquad (2.5)$$

ACI code restricts the spacing between shear reinforcement to half of effective depth or 24 inches for non pre stressed members. This condition ensures interception of potential diagonal crack by at least one vertical stirrup.

2.6.1 Diagonal Crack Width and Minimum Shear Reinforcement

When the principle tensile stress at some location reaches the cracking strength of concrete, a crack is formed in the concrete. This crack is normal to the direction of principal tensile stress. In case of members under pure axial tension or to pure flexure, the principal tensile stresses are parallel to the longitudinal axis of the member and cracks form perpendicular to the member axis. The principle tensile stress directions are inclined to the longitudinal axis of the member if the cross section of a member is subjected to shear stresses. A crack is formed at a location where significant shear stresses exist, and is inclined to the member axis. Such cracks are termed as diagonal cracks.

The inclination, spacing and width of the diagonal cracks cannot be predicted by calculating principle stresses in un cracked beam, rather, it depends on many factors including flexural and shear reinforcement ratios, size and shape of cross section, shear stresses and mechanical properties of concrete and steel. This implies that the inclined cracking width can be calculated using empirical equations, based on empirical works only (Jensen / Lapko 2009)

`
[20]. Various research studies as mentioned below have been carried out to find the empirical expression for determining crack widths.

- Placas and Regan (1971) [21] concluded that maximum crack width is directly proportional to spacing of stirrups and inversely proportional to A_v, $(f'_c)^{1/3}$ and d.
- Bentz, Vecchio and Collins (2006) [22], reasoned out in MCFT that crack width is equal to the product of crack spacing and principal tensile strain.
- More recently, Muttoni and Ruiz (2008) [23] stated that critical crack width is proportional to the product of longitudinal strain in the control depth ($0.6\ d$) times effective depth of element.

2.7 Zararis Theory of Critical Shear Crack

Prodromos D. Zararis[5] has carried out a comprehensive and systematic research on shear behavior of reinforced concrete slender beams both with and without shear reinforcement under concentrated loads as well as uniformly distributed loads (UDL) and evolved a theory which describes the diagonal shear failure in slender beams. The theory has also been compared with the known experimental results. This theory explains the shear behavior of beams and provides empirical equations to determine the ultimate shear capacity and minimum shear reinforcement for reinforced concrete slender beams required to restrain the growth of diagonal cracking and prevent a brittle failure.

2.7.1 Beams without Shear Reinforcement

In slender beams loaded under two or single point loading, failure occurs due to critical diagonal crack. Such crack is composed of two distinct branches as in Figure 2.11. First one is an inclined shear crack having height almost similar to flexural cracks. The second branch initiates from the tip of the first branch and propagates towards the load point crossing the compression zone, with its line meeting the support point (Figure 2.12). Second branch which also involves splitting of compression zone concrete is believed to be responsible for failure. This splitting is not similar to the one occurring in the common split cylinder test.

`

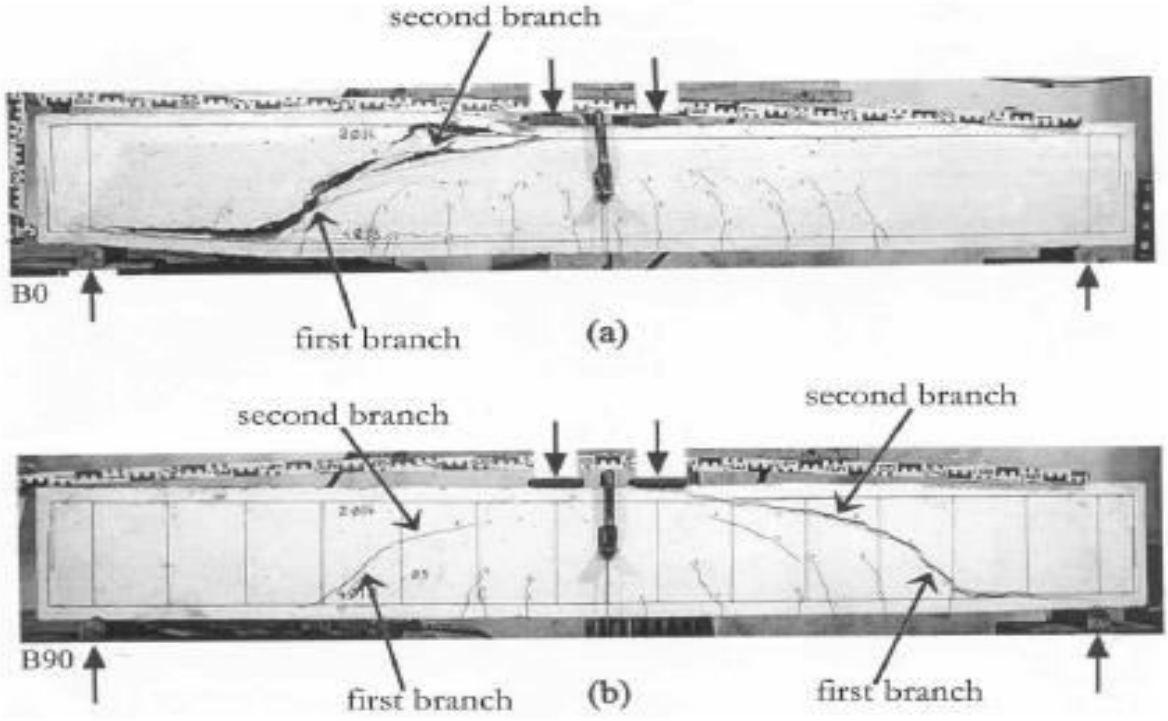

Figure 2-11 Cracking pattern of slender beams

Nominal shear stress 'v_{cr}' at diagonal tension cracking can be calculated by a simple expression derived in this research as $v_{cr} = V_{cr}/bd = (c/d)f_{ct}$. Moreover, to cater for the size effect on the shear strength, it introduces a correction factor as under:-

$$v_{cr} = \frac{V_{cr}}{bd} = (1.2 - 0.2(\frac{a}{d})d) * (\frac{c}{d}) f_{ct} \qquad (2.6)$$

where,

$$1.2\text{-}0.2(a/d)d \geq 0.65 \text{ (d in m)}$$

Taking into account that $a = (a/d)d$, the size effect in beams appears to depend not only on the depth d, as is commonly believed, but also on the ratio (a/d).

`

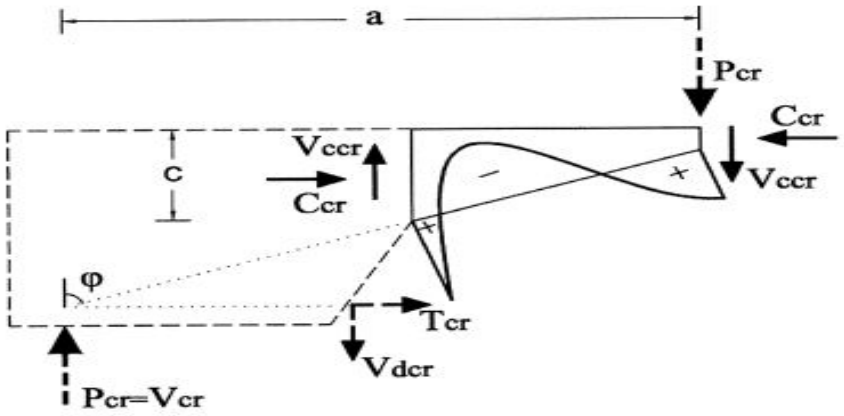

Figure 2-12 Stress distribution along line of splitting (+: tension, -: compression)

On formation of second branch, dowel force in longitudinal reinforcement 'V_{dcr}' significantly increases. This results in horizontal cracking of concrete cover along main reinforcement. This cracking finally causes loss of 'V_d'. At this point, complete shear force is resisted by compression zone concrete which eventually fails because of shear as shown in Figure 2.11a.

2.7.2 Beams with Transverse Reinforcement

The pattern of cracking of slender beams with stirrups is similar to that of beams without stirrups. The critical crack, in both cases, typically involves two branches, which are formed in the same region of beams. It is reasonable to consider that the causes of formation of the second branch as well as the corresponding cracking load are identical in both cases. Up to the formation of the second branch, the effect of stirrups can be considered negligible. When the formation of the second branch is complete, the concrete shear force V_{ccr} in the compression zone above the beginning of the second branch is equal to that at the second branch. The same also occurs for the concrete compression force C_{cr} as shown in Figure 2.12. In this figure, the normal force T_{cr} and the shear force V_{dcr} of the longitudinal steel bars (by the cracking of the second branch) are also depicted. By the cracking of the second branch of the critical crack, the stirrups are brought into action. The gradual opening of the second branch, from the tip of the first branch towards the load point, requires a gradual increase of the concrete shear force V_{ccr} at the beginning of the second branch to balance the developed force V_s of stirrups.

Moreover, the opening of the second branch of critical crack causes an increase ΔV_d in the shear force of the longitudinal steel bars. However, it is important to note that its existence

`

is only due to inclusion of stirrups. Thus, the forces acting at failure on the portion of the beam above the critical diagonal crack can be considered to be those shown in Figure 2.13.

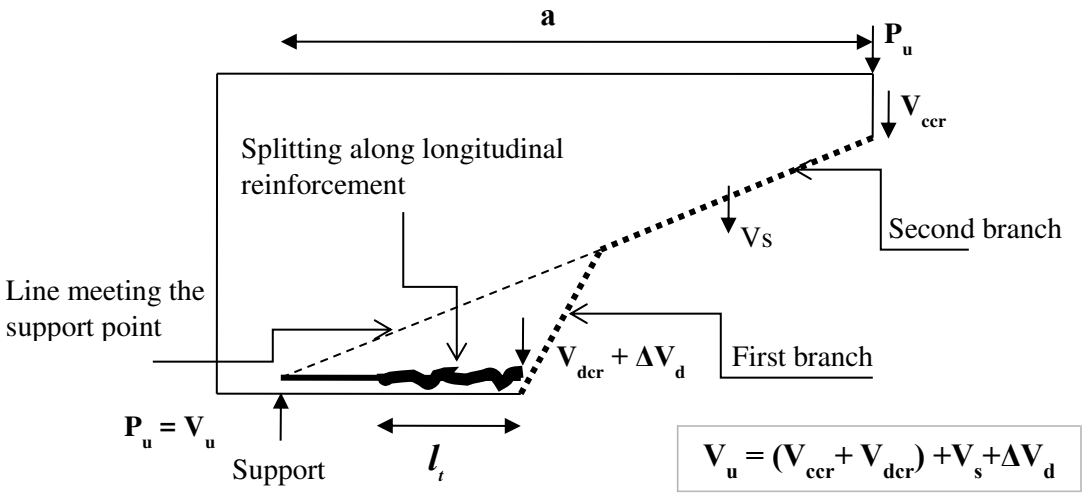

Figure 2 13 Distribution of forces in beam (based on Zararis theory).

Shear force, V_{cr} at the beginning of cracking of second branch is the sum of the dowel force in longitudinal reinforcement, V_{dcr} and shear force in concrete at the time of cracking, V_{ccr} *i.e.* $V_{cr} = V_{ccr} + V_{dcr}$. Then, through the vertical equilibrium of forces;

$$V_u = V_{cr} + V_s + \Delta V_d \qquad (2.7)$$

Although yielding of stirrups at least at the location of critical crack is an important condition for shear failure, however, mere existence of this condition is not sufficient. The shear failure of a slender beam is caused only when, in addition to the yielding of stirrups, the shear force of longitudinal steel bars, V_d brings about a horizontal splitting of concrete cover along the longitudinal reinforcement. This splitting results in the loss of the shear force V_d and, consequently, the failure of beam. Preventing this splitting hinders the shear failure. It has been assumed that splitting is caused when the tensile stresses developed along the reinforcement in a distance l_t from the point of initiation of critical crack exceeds the tensile strength, f_t of concrete. Forces acting in the region of horizontal splitting are depicted in Figure 2.14.

`

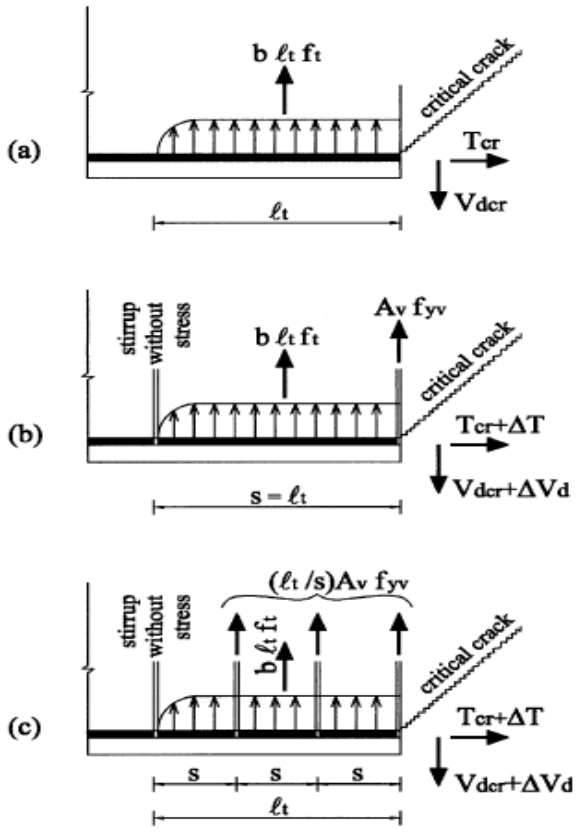

Figure 2-14 Forces acting in the region of horizontal splitting along the longitudinal reinforcement of beam (a) without stirrups, (b) with stirrups at spacing, s= lt and (c) with s< lt

This splitting length l_t has been believed to have a constant value in any case which is of the order of 0.5d. Taking into account the values for V_{cr}, V_s and $\Delta V_{d,}$ the final equation proposed by Zararis for ultimate shear capacity V_u of beams with stirrups, in its complete form, is as under:-

$$V_u = [(1.2 - 0.2(\frac{a}{d})d)(\frac{c}{d}) f_{ct} + (0.5 + 0.25(\frac{a}{d}))\rho_v f_{yv}]bd \qquad (2.8)$$

2.7.3 Minimum Shear Reinforcement

The manner of splitting along the main reinforcement implies a gradual increase in force V_d in longitudinal steel, accompanied by a gradual increase of the force in stirrup until yielding occurs. The increase in force in longitudinal steel, ΔV_d can be much larger than the one required for yielding of stirrups. This force, surplus to the one required for the onset of yielding of stirrups, is actually responsible for the horizontal splitting. This force was calculated in two

`

different terms i.e. forces acting along the splitting length l_t (equation 2.9), and the distribution of shear stress along main reinforcement and the axial stress of stirrups (equation 2.10)

$$\Delta V_d = 0.5\rho_v f_{yv} bd \qquad (2.9)$$

And,

$$\Delta V_d = 0.28(\frac{\rho/\rho_v}{a/d}) f_{yv} bd \qquad (2.10)$$ The minimum amount of shear reinforcement commonly corresponds to a value that restrains the growth of inclined cracking, providing an increased ductility and preventing a sudden shear failure. To avoid undesirable widening of the critical diagonal crack (as well as that of the horizontal splitting crack), a surplus of the force ΔV_d must not exist. This occurs when the value of ΔV_d given by Equation 2.9 equals the one given by Equation 2.10. Equating these two equations, the ratio ρ_v of shear reinforcement, in relation to the ratio ρ of main tension reinforcement, must satisfy the following equation:-

$$\frac{\rho}{\rho_v} \leq 1.75(\frac{a}{d}) \qquad (2.11)$$

Equation 2.11 constitutes the criterion that the minimum shear reinforcement must fulfill. When the ratio $\rho/\rho_v > 1.75(a/d)$, the shear failure of a beam is accompanied by a quick and extensive splitting crack along the longitudinal reinforcement, as well as by significant widening of the critical crack.

2.8 Modification in Zararis Theory

Zararis considered that the splitting length, l_t has a constant value which is about 0.5d. It is believed that this splitting length is linked with the development length, l_d of the bars. This concept is based on the fact that the factors influencing the development length are similar to those linked with the splitting length along main reinforcement. Purpose of providing development length is to enable the bars to attain average bond stress over length of embedment so that splitting of highly stressed bars is avoided. According to ACI Code, the development length is influenced by size, location and number of bars, concrete cover, coating on the reinforcement, confining reinforcement, yield strength of steel and compressive strength

`

of concrete. These factors are also thought to be the influencing the splitting length as described above. Therefore, instead of relating splitting length, l_t with the depth of a beam only, it would be more appropriate to relate it with some fraction of the development length, l_d. Exact value of this fraction may be found by experimental studies, however, for the purpose of this research, it has been assumed that splitting length is 0.25 times the development length for these beams.

By incorporating the above mentioned assumption, Equation 2.9 becomes:-

$$\Delta V_d = 0.25(\frac{l_d}{d})\rho_v f_{yv} bd \qquad (2.12)$$

Now by equating the Equations 2.10 and 2.12, the ratio ρ/ρ_v for minimum shear reinforcement becomes:-

$$\frac{\rho}{\rho_v} \leq 0.89(\frac{l_d}{d})(\frac{a}{d}) \qquad (2.13)$$

Similarly, using the value of splitting length l_t = 0.25 l_d, the Zararis equation for predicting ultimate shear strength of reinforced concrete slender beams can be modified as under:-

$$V_u = [(1.2 - 0.2(\frac{a}{d})d)(\frac{c}{d}) f_{ct} + 0.25((\frac{l_d}{d}) + (\frac{a}{d}))\rho_v f_{yv}]bd \qquad (2.14)$$

`

EXPERIMENTAL PROGRAM

3.1 GENERAL

This chapter explain the methodology of experimental program which is carried out to get the objective of this research. For this purpose eight full scale beams, two without shear reinforcement, two with ACI equation for minimum shear reinforcement (Equation 2.4), two with Zararis minimum shear reinforcement (Equation 2.8) and two with Modified Zararis minimum shear reinforcement (Equation 2.14) were cast and tested to study the shear behavior of these beams.

3.2 Materials

3.2.1 Cement

The Type I cement conforming to ASTM C 150 – 04 was used. Results of the tests carried out to ascertain the properties of cement are presented in Table 01 (Appendix I).

3.2.2 Fine Aggregate

Locally available sand (from Lawrencepur) with fineness modulus of 2.6 and specific gravity of 2.697 was used. Results of the tests conducted for verification of properties of sand are shown in Table 02(Appendix I). The gradation of the fine aggregate is tabulated in Table 03 (Appendix I), and graphically shown in Figure 2(Appendix I).

3.2.3 Coarse Aggregate

Aggregate procured from Margalla crush site was used in this research. Maximum size for the aggregate was kept as 19 mm. For gradation purpose, five sizes i.e. 25 mm, 19mm, 12.5mm, 9.5 mm and 4.75mm were considered i.e.12.7 mm, 9.5 mm, 4.75 mm. The specific gravity of coarse aggregate was found 2.685 The laboratory test results are tabulated in Table
04(Appendix I). The gradation and sieve analysis was determined in accordance with ASTM C 136 – 01 and tabulated in Table 05 (Appendix I) and graphically shown in Figure 3 (Appendix I).

`

3.2.4 Reinforcing Steel

The grade 60 and grade 40 mild steel was used for longitudinal and transverse reinforcement respectively. For longitudinal tensile reinforcement # 9 bars were used and #5 size bars were used for compressive reinforcement. #2 and #3 bars were used as transverse reinforcement. Test result of reinforcement bar was shown as Figure 1(Appendix I).

3.2.5 Superplasticizers

Super plast 470 (product of Ultra Chemical Company), a high performance concrete superplasticizer based on modified poly carboxylic ether, was used in the research. The plasticizer was used to increase workability of mixture. The dosage was kept constant throughout the research work as 0.9% by weight of cement. The technical data of Super plast 470 is tabulated in Table 06(Appendix I).

3.2.6 Water

Potable water was used for mixing as well as curing of concrete.

3.2.7 Mix Design

Concrete mix was designed for a 28 day concrete strength f'_c of 4000psi. The average concrete cylinder strength tested at the day of testing was 4118 psi. The results are tabulated in Table 07(Appendix I).

3.3 Casting of Specimens

Specimens were cast as per ASTM C 31 and 31M. Eight beams were prepared with single batch of concrete procured from a batching plant. 12 cylinders (6''x12") were casted to determine the compressive strength of concrete.

3.3.1 Test Specimens

For this experiment eight beams were casted having constant rectangular section of 10'' wide18" deep with effective depth of 16" and 120 inch in length .Specimens were cast as per ASTM C 31 and 31M.Beam sizes and properties was so selected that minimum shear reinforcement requirement is governed by empirical equation 2.4 and spacing requirement

`

by equation 2.5. The longitudinal tensile reinforcement for all beams were kept constant as 1.866 % .The beams were divided into four series based upon the amount of shear reinforcement. N- Series had no shear reinforcement, whereas A- series had minimum amount of shear reinforcement as specified by ACI 318-08. Z- Series contain minimum amount of shear reinforcement as proposed by the Zarari's and mentioned in equation 2.11. M- Series had minimum amount of shear reinforcement as per the modified Zarari's equation as mentioned in equation 2.13. The specimen specification and material properties are shown in Table 08(Appendix I) and presented diagrammatically in Figure 4(Appendix I).

3.3.2 Sample Preparation

The concrete was mixed at batching plant in Rawalpindi and then brought to the site (SCEE, NUST) using transit mixer. The beams were cast as per ASTM C 31/31M. Steel shuttering plates made of a steel were used for casting of beams in order to get good result. The size of the steel plate was (48"x18"). The concrete was then poured manually into the formwork. Mortar spacer tied with 1 ''bars was used to maintain a minimum clear cover. A vibrator is used to ensure that a pour is even and free of air bubbles so that concrete will remain strong and have a smooth finish even after formwork is removed. The formwork was then removed after 24 hours and wet hessian cloth was wrapped around the specimens for curing. The curing was done in open environment whereas the cylinders were cured in water tank for 28 days. Beam form work is shown in Figure 7(Appendix 1).

`

3.4 Testing of Specimen

With the help of a crane the beams were then shifted to the SCEE NUST Lab as shown in Figure 5(Appendix 1).

3.4.1 Test Setup

The specimens were subjected to a load which was applied through a hydraulic jack having a capacity of 120 ton .Load cells were attached to a reaction frame which was used to measure the applied load. Fork lifter was used to lift the beam and placed the beam on the supports. The load was applied to the beam using a remote control device. For this experimental study load was applied using remote control in increments of 2.5 tons which was displayed at the display panel. Steel girder was used to apply two point load. Three LVDTS were used to measure the deflection of beams. The deflection was recorded through structural load analysis and automation system. Test set up is shown in Figure 6(Appendix A).

3.4.2 Test procedure

Beams were placed under two point loading. A steel plates were placed at a distance of 40 inch from both sides of the support making a two point loading system. The beams were centered and align on rigid support using a fork lifter. The support was adjusted according to the length of a beam and specimen was loaded using a 120 ton jack. Deflection of beam was measured using three LVDTS one at the center of span of beam and other two at the L/3 from the support . Load was applied in increments of 2.5 ton and cracks were observed and marked on the beam surface using permanent marker. This process was repeated until the beam reached its ultimate capacity. The average response of two beams tested in a series was taken as the representative response of the corresponding series.

EXPERIMENTAL RESULTS

4.1 General

This chapter summarizes the results obtained from the beams tested in experimental program. For experimental program beams were casted at NUST University and the result obtained from these tests are summarized in this chapter. Load was applied gradually and deflection was measured with the help of LVDT'S. The result include the behavior of crack propagation and ultimate shear strength of beam.

4.2 Deflection

The LVDT‟s were used to measure the deflection of beams. Three LVDT‟s were placed under the beam and were connected to the computer based structural load analysis and automation system (Made by National Instruments (USA) and assembled locally) which is shown in Fig. 1(Appendix II). The deflections against each load was measured by LVDT‟s and automatically stored in computer as a text file by software (Lab view) based data acquisition system. The detailed values of deflections against loads are shown in Appendix II.

4.3 Concrete Strength

Twelve cylinders of concrete were cast and tested as per ASTM C 39.Three cylinders were tested at 7days, 3 cylinders at 14 days and 3 cylinders at 28 days respectively. The remaining 3 cylinders were tested at the day of testing of the beams. The compressive strength comes out as 4148 psi.

4.4 Behavior of Test Specimen

All beams was carried out at SCEE, NUST Laboratory on 5th May 2015. The sample was loaded at two points with span to depth ratio (a/d) of 2.5 and load rate of 2.5 Ton per increment. After each increment the cracks were noted and marked, deflections were measured and stored automatically by digital data logging system. The behavior of the specimens till failure is as under.

`

4.4.1 Specimen N-1

No visible cracks appeared in the beam up to a load of 5 ton. Flexural crack started at 8 ton close to the mid span of the beam. More flexural cracks appeared at a load of 12.5 ton .With increase in load up to 17.5 ton the flexural cracks increased in number and the crack which appeared earlier propagated upwards perpendicular to the web of beam. When a load reached at 22.5 ton a sudden diagonal crack appeared near to the support. At 27.5 ton cracks widen up and cracks propagates both in forward and backward direction. At 32 ton beam suddenly fails in shear due to inclined cracks with a breaking sound. . The observed inclination of first branch crack was 45 degree with respect to the axis of the beam followed by 25 degree from mid web to load point.

Load Deflection s tabulated in Table 01(Appendix II) and the Plot is shown in Fig 02 (Appendix II). Cracking pattern of beam is shown in Fig 03(Appendix II).

4.4.2 Specimen N-2

No noticeable cracks appeared till 7.5 ton .Flexural cracks started appearing at 10 ton on the middle portion of a beam. More flexure cracks appeared at 12.5 ton. Up to 17.5 ton the flexural cracks increases in number as well in size and propagated upward perpendicular to the axis of beam. At 20 ton a large diagonal crack appeared which starts propagates towards the support. At 25 ton another inclined cracks appeared starting from the same origin and the cracks propagates in backward direction. At 27.5 ton the cracks widens up. At 30 ton beams suddenly fail in shear due to inclined cracks .The observed inclination of first branch was about 47 degree with respect to the axis of beam up to the mid web followed by 22 degree from mid web to load point.

Load Deflection data is tabulated in Table 02 (Appendix II) and Plot is shown in Fig 04 (Appendix II). Cracking pattern of beam is shown in Fig 05(Appendix II).

.

`

4.4.3 Specimen A-1

No cracks was noticed till 7.5 ton load. At 11.5 ton flexural cracks started at mid span of beam. At 12.5 ton flexural cracks increased in number as well as in size. At 15 ton the flexural cracks propagated vertically upward. Till 17.5 ton load the flexure cracks grew more in number. At 20 ton inclined cracks appeared towards left side of support. At 25 ton the major inclined cracks started propagating towards the load and major inclined cracks also appeared towards the westward side of the beam. At 28 ton the cracks propagated towards the load point from both sides of the beam. At 30 ton more inclined cracks appeared near the support. At 33 ton a distinct branch of shear crack propagated both in forward and backward direction. At 37.5 the inclined cracks widened up. At 40 ton the beam failed in shear due to inclined cracks .The observed inclination of first branch was about 47 degree with respect to the axis of beam followed by 31 degree from mid web to a load point.

Load Deflection data is tabulated in Table 03(Appendix) and the Plot is shown in Fig 06 (Appendix II). Cracking pattern of beam is shown in Fig 07 (Appendix II).

4.4.4 Specimen A-2

Initial vertical crack appeared in the center of beam at a load of 7.5 tons. With further increase in load, more flexure cracks appeared at the middle portion of the beam. At 17.5 ton load the flexure cracks increases in number as well as in size and propagates vertically upward .At 22.5 ton major inclined cracks appear towards left side of support. At 27.5 ton these inclined cracks starts propagates towards the load point. At 30 ton more inclined cracks appear near the support. At 32.5 the inclined cracks starts propagates towards the load point. At 35 ton a distinct branch of shear crack propagates backward towards the support and also propagates forward towards the load point. At 37.5 crack widens. At 42.5 the beam fails in shear due to inclined cracks. The observed inclination of first branch was about 45 degree with respect to the axis of beam followed by 24 degree from mid web to load point.

Load Deflection data is tabulated in Table 04(Appendix) and the Plot is shown in Fig 8 (Appendix II). Cracking pattern of beam is shown in Fig 09 (Appendix II).

`

4.4.5 Specimen Z-1

No flexure cracks appeared in the beam at a load of 10 ton. At 12.5 ton flexure cracks starts to appear at middle portion of the beam. At 15 ton more flexure cracks appeared near the support at a distance of L/3 from the support. At 17.5 ton flexure cracks increased in number as well as in size. At 22 tons flexure crack appeared at a distance of L/3 from support started inclined towards the load point. More flexure shear cracks appeared near the support at a load of 30 ton. At 32.5 ton flexure cracks appeared near the support starts inclined towards the load. At 35 ton these inclined cracks propagated towards the load point. It has been also seen that flexure cracks also propagated upward when load was increased from 32 ton .Inclined cracks started to converge at 50 ton towards the load point. At 55 ton the cracks increased in length and also widened up. At 67.5 beam fail in shear due to diagonal crack.

Load Deflection data is tabulated in Table 05(Appendix) and the respective Plot is shown in Fig 10 (Appendix II). Cracking pattern of beam is shown in Fig 11 (Appendix II).

4.4.6 Specimen Z-2

No visible cracks appeared at a load of 7.5 ton. Vertical cracks appeared at the center of beam at a load of 10 ton. At 12.5 ton more flexure cracks developed at the mid span of beam. At 15 ton flexure cracks started propagating vertically upward from bottom of the beam .At 30 ton flexure cracks appeared near the support started inclined towards the load .At 33 ton more number of inclined cracks appeared near the support. At 40 ton inclined cracks kept propagating towards the load. At 47.5 these inclined cracks starts converged towards the load point. At 55 ton the crack widens up and cracks increase in length .At 61 ton beams fail due to the diagonal shear crack.

Load Deflection data is tabulated in Table 06(Appendix II) and the Plot is shown in Fig 12(Appendix II). Cracking pattern of beam is shown in Fig 13 (Appendix II).

4.4.7 Specimen MZ-1

No flexure cracks seen up to a load of 7.5 ton. Flexural cracks appeared at 10 ton load,2h/3 at a distance from left side of support .At 15 ton these flexure cracks propagated vertically upward. At 17.5 ton the flexural cracks grew in number as well as in size .At 30 ton

`

flexure cracks near the support started inclined towards the load point. At 32 ton these cracks started propagating towards load point. At 47.5 more number of inclined cracks developed. At 50 ton major inclined cracks started propagating in backward direction towards the support and also propagated forward towards the load point. .The flexure shear cracks started getting close to each other and started to converge towards the load point. At 50 ton inclined cracks reached towards the load point. At 52 crack started widening. The cracks kept widening until failure occurred at 57.5 ton. Failure is due to the diagonal shear cracks.

Load deflection data is tabulated in Table 07 and the plot is shown in Fig 14 Appendix II. Cracking pattern of the beam is shown in Fig 15 Appendix II.

4.4.8 Specimen MZ-2

Flexure cracks started appearing at 10 ton at the center of the beam .At 12.5 ton more flexure cracks were appeared near the support. Up to 17.5 ton these flexure crack increased in number and propagated vertically upward. At 20 ton major inclined cracks developed on left side of support. At 30 ton these cracks propagated towards the load point. At 30 ton inclined cracks which is developed near the support started inclined towards the load point. At 32.5 inclined cracks started getting close to the first inclined crack and propagated towards the load point At 45 ton backward propagation of inclined cracks were also observed towards the support along with forward propagation towards the support. At 47.5 the inclined cracks reached towards the load point .At 50 ton the cracks widened up. Ultimately at 52.5 ton the beams fails due to diagonal shear crack

Appendix II. Load deflection data is tabulated in Table 08(Appendix II) and the plot is shown in Fig 16 (Appendix II). . Cracking pattern is shown in Fig 17(Appendix II).

`

4.5 Experimentation Summary

- All beams exhibit similar crack pattern and mode of failure is shear failure.
- Initial cracks were observed at mid span of beam, perpendicular to the axis of beam. These are flexure cracks which were observed initially at about 15 to 30 percent of the ultimate shear failure.
- With further increase in load new flexure cracks were observed which is away from the mid span of beam and towards the support.
- The vertical cracks grew away from the load point, tend to inclined towards the load point when load applied to around .35 to .6 Pu. These are flexure shear cracks. In A-series these are around 0.5 to 0.6 Pu, M-series these are at 0.4 to 0.5 Pu, Z-series these are at 0.35 to 0.45 Pu.
- The flexure shear cracks and pure shear cracks kept propagating towards the load point until the beams fail in shear. However flexure cracks growth was reduced when flexure shear cracks appeared.
- Two distinct branches of critical diagonal shear cracks were also witnessed as observed by P. D. Zarari which is prominent in A-series .However in Z-series and M-series no distinct branches of critical diagonal shear cracks were observed.
- Splitting of concrete along longitudinal reinforcement was witnessed in A-series.
- In Z and M series beams no splitting of concrete along longitudinal reinforcement was witnessed.

TEST RESULT ANALYSIS, DISCUSSIONS AND CONCLUSIONS

5.1 General

This experimental program was devised to study the shear behavior of reinforced concrete slender beams at a/d of 2.5 and having moderate longitudinal reinforcement. Beams were classified into four different categories based on the minimum amount of shear reinforcement provided according to existing and established guidelines. The influence and efficiency of this variation in amount of transverse reinforcement was observed from the experimental shear strength values of these beams. Cracking patterns and failure mechanisms were also studied.

5.2 General behavior of Beams

Beams with no shear reinforcement showed sudden failure due to diagonal cracks. These cracks propagated from the support and extended up to the point of beam. The failure of N-series beams were caused by excessive widths of shear cracks. Backward propagation of cracks along with the longitudinal reinforcement up to the support was also observed in beams. Sudden load drop was observed in N-series as compared to Z-series, A-series and M-series.

Beams with ACI specified minimum shear reinforcement (A-Series), failed due to diagonal shear cracks. Splitting of concrete along longitudinal reinforcement was also witnessed in A-series. A number of other diagonal cracks were witnessed in the beam web in addition to the major diagonal crack which widened appreciably at failure.

Beam with minimum shear reinforcement as per Zarari's failed relatively at large loads. In Z-series, two distinct branches of diagonal cracks were not observed as postulated in the theory. Diagonal shear cracks occurred at relatively greater load than A-series beam. In Z-series several diagonal cracks were witnessed which propagated towards the load point. This series exhibited maximum deflections as compared with other beams.

The beam with minimum steel reinforcement as specified by modified form of Zarari's equation (M-series) shows a similar behavior as that of a Z-series but fail at a lesser load. The crack pattern of Modified Zarari's was much similar to the Z-series. The deflections in these series were more than A-series and N-series but less than Z-series.

`

5.3 Load deflection response

Load deflection response of beams are shown in Figure 01(Appendix III). Deflection at center of beam was plotted against the applied load. It was observed that deflection increased with increasing loads up to the failure of beam. After reaching the failure there was drop in the load but the deflection continues to increase .The maximum deflection was noted at loads of 70% to 82% of maximum load beyond the peak. M-series, Z-series and A-series behaved in a ductile manner except N-series where sudden failure occurred. The deflections at mid span of beam of all series were then compared with theoretical cracked and un cracked deflection .Initial load deflection followed the theoretical values .The majority of experimental deflection lies between the theoretically calculated cracked and un cracked sections. It can be justified by postulating that theoretical cracked deflection are calculated assuming the section is fully cracked which is not in reality .It was observed that the section is fully cracked which is not in actual case. It has been observed that the specimens with more shear reinforcement displayed larger deflections before failure. The detail load deflection plots of each specimen are shown in Appendix II.

5.4 Modulus of Rapture of Concrete

Modulus of rapture of concrete is determined by using the general expression

$$fr = \mu\sqrt{f'c}$$

Different researchers have proposed different value for μ . The value of 7.5 has been adopted by ACI for normal weight concrete. The theoretical value of fracture stress using ACI equation was found to be 482 psi and corresponding load is 12.63Kips. In this experimental program, the cracking stress of specimens were observed between 490 psi to 770 psi which the corresponding loads were 17 to 22 kips. The values of μ lied between 7.7 and 12. The data is tabulated in Table 1 (Appendix III).

`

5.5 Shear strengths of Specimens

Theoretical shear strength of beams was calculated using ACI 318-11 (11-2) equation (A-series). Zarari's proposed equation (2.22) (Z-Series) and Modified form of Zarari's equation (2.28) (M-Series) and were compared with the experimental values. The comparison of experimental and theoretical shear strength is given in Table 02(Appendix III) and graphically presented in Figure 02 (Appendix III). From Figure 02 it can be concluded that that Modified Zarari Equation is the most accurate and close value .ACI equation is understandably conservative in predicting the shear strength of concrete. ACI equation does not account for the contribution of dowel action, aggregate interlock between shear cracks, and shear span to depth ratio. Variation in experimental shear strength from ACI theoretical calculated shear strength is graphically shown in Figure 03 (Appendix III) .The comparison of experimental shear strengths with Zarari and Modified Zarari predicted shear strength were graphically presented in Figure 06 and Figure 07(Appendix III) . It is observed that predicted shear strengths of Zarari's equation is close to the experimental value and its percent variation is between 10 to 27 percent. Modified Zarari equation is even close to the experimental value and its percent variation is only between 0 to 20 percent.

.

The concrete shear strength depends upon various factors such as contribution from dowel action, aggregate interlock along diagonal crack and shear in compression zone of a concrete. Shear strength provided by concrete (Vc) is predicted by ACI Eq. 11.3 by the relationship, $Vc = 2\sqrt{f'c}\ bd$, where all the contributions are considered lumped and fixed as 2 which is not right. The value of factor γ was calculated from experimental results. Values of factor γ obtained in this study were 3.43, 3.71, 4.09 and 3.96 for N, A, Z and M-series respectively which are tabulated in Table 03 (Appendix III) and graphically illustrated in Fig 05 (Appendix III). It was observed that with increase in transverse steel ratio, the value of γ increased which can be attributed to the fact that presence of stirrups in concrete controls the crack width and also controls the concrete splitting along the longitudinal reinforcement which was discussed in literature review .Variation in concrete contribution from ACI predicted strength is shown in Fig 04 (Appendix III) .It is clear that the amount of transverse steel adds the shear strength of concrete.

`

5.6 Achieved Moment Capacity of Specimens and Minimum Shear Reinforcement.

Experimental moment capacities for each beam were calculated by multiplying the ultimate load "Vu" at each loading point with the shear span "a". Nominal moment capacity of the specimens were calculated using ACI equation, $M_n=A_s f_y(d - 0.5a)$. Shear failure of members is generally brittle and sudden. Therefore, the members are designed to ensure that member should not reach the ultimate shear capacity before flexural capacity. It is clear from Figure 09 (Appendix III) that with increase in transverse steel ratio, the shear strength increases. Although shear reinforcement is not taken into account in the flexural strength calculation of RC beams. It was observed that the increase in shear reinforcement enhance the flexure capacity of the beams. Relationship between ratio of the experimental to theoretical moment capacity and transverse steel ratio is given in Figure 08 (Appendix III).

. Experimentally achieved flexural capacity of N, A, M, and Z-series beams was 53.29%, 69.5%, 92%, and 105% of theoretical moment capacity respectively. Tests on the beam specimens revealed that Zarari's equation and its modified form provided better results by using more amount of minimum shear reinforcement as compared to ACI equation and achieves greater failure loads and better ductility. Therefore it can be concluded that the minimum amount of shear reinforcement proposed by Modified Zarari equation may be used to achieve theoretical nominal moment capacity.

`

.

5.7 Modifications to Zarari Equation

Zarari postulate that the splitting length, lt has constant value of about 0.5d.In this experimental program, equations developed by Zarari were modified to take into account the development length. It has been assumed that splitting length, lt as shown in Figure 2.13, should be a multiple, α of the development length (ld)of bars. The value of α was assumed to be 0.25 in this study. This provided a value of 0.0031 for Pv and accordingly the M-Series beams were equipped with this amount of transverse steel. It is believed that minimum shear reinforcement should be such that it should allow the beam to attain 100% of the designed flexural capacity. Figure 5.3 illustrates that for 100% flexural capacity, corresponding value of ρv is 0.0038. For getting this value of ρv from Equation 2.13, the factor α should be taken as 0.165. To keep a safety margin, the factor for development length has been multiplied by 0.9 which reduces it to 0.15 i.e. lt = 0.15ld. By incorporating this value, Equations 2.13 and 2.14 are respectively amended as under:

.

$$\frac{\rho}{\rho_v} \le 0.53(\frac{l_d}{d})(\frac{a}{d})$$

$$V_u = [(1.2 - 0.2(\frac{a}{d})d)(\frac{c}{d}) f_{ct} + 0.15(\frac{l_d}{d}) + 0.25(\frac{a}{d}))\rho_v f_{yv}]bd$$

`

5.8 Conclusions

Eight reinforced beams were tested with moderate longitudinal reinforcement ratio and span to depth ratio (a/d) of 2.5.Following conclusion can be drawn from the experimental values and the analysis of test results.

- ACI 318 equation is conservative in predicting the ultimate shear strength of beam. Zarari equation and Modified form provides better results.
- Increase in transverse reinforcement increases the maximum deflection in beams and also increases the ductility of beam.
- Zarari's minimum transverse reinforcement ratio achieves the theoretical moment capacity of beam whereas ACI and Modified Zarari fails prior to achieve theoretical nominal moment capacity of beam with moderate longitudinal reinforcement.
- Splitting of concrete along longitudinal bar is significant in beams with less shear reinforcement. Splitting of concrete along longitudinal reinforcement can be controlled by providing minimum amount of transverse reinforcement ratio as specified by P.D.Zarari.

`

5.9 Recommendations

Some of the recommendations for future studies are summarized as under:-

- More experimental work is required to understand the shear behavior of reinforced concrete beams.
- Additional experimental studies are required to established minimum shear reinforcement ratio to attain nominal moment capacity
- Experiment needs to be done to evaluate the effect of span to depth ratio and longitudinal reinforcement on ultimate shear strength.
- Further experimental work needs to be done to evaluate the contribution of concrete in ultimate shear strength by varying transverse reinforcement ratio.
- Effect of cracking width and crack pattern should also be investigated .

`

Appendix-I

Table 1: CEMENT PROPERTIES

Tests	**Test results**	**Specifications**
Specific gravity	3.15	ASTM C 188 – 95
Initial setting time	170 minutes at 17^{0}C	ASTM C 191 – 01
Final setting time	330 minutes at 17^{0}C	ASTM C 191 – 01

Table 2: PROPERTIES OF FINE AGGREGATE

Tests	**Test results**	**Specifications**
Specific gravity	2.60	ASTM C 128 – 01
Absorption	1.1%	ASTM C 128 – 01
FM	2.45	ASTM C 33 – 02

Table 3 : GRADATION OF FINE AGGREGATE

Sieve No	**Weight Retained (gm)**	**Percent Retained**	**Cumulative Percent Retained**	**Percent Passing**	
				Actual	**ASTM C 33 – 02**
#4	2	0.2	0.2	99.8	95 – 100
#8	16	1.6	1.8	98.2	80 - 100
#16	134	13.4	15.2	84.8	50 - 85
#30	320	32	47.2	52.8	25 - 60
#50	425	42.5	89.7	10.3	5 - 30
#100	70	7	96.7	3.3	0 - 10
#200	31	3.1	99.8	0.2	
Pan	2	0.2	100	0	

`

Table 4: PROPERTIES OF COARSE AGGREGATE

TEST DETAILS	TEST RESULTS
Impact value (percent)	11.4
Crushing value(percent)	21.4
Abrasion value(percent)	15.8
Specific gravity	2.60

Table 5: COARSE AGGREGATE GRADATION

Sieve Size (mm)	Weight Retained (gm)	Percent Retained	Cumulative Percent Retained	Percent Passing	
				Actual	ASTM C 33 - 02
19	0	0	0	100	100
12.5	78	7.8	7.8	92.2	90 - 100
9.5	410	41	48.8	51.2	40 - 70
4.75	488	48.8	97.6	2.4	0 - 15
2.36	24	2.4	100	0	0 - 5

Table 6: HIGH RANGE WATER REDUCING AGENT. (TECHNICAL DATA)

DESCRIPTION	DETAILS
Name	Ultra Superplast 470
Form	Viscous liquid
Color	Brown
Specific gravity	1.190 at 20^0C
Alkali content (%)	Typically less than 72.0 g
Chloride content (%)	Nil to BS 5075
Air Entrainment	Less than 2%

`

Sr#	Age Days	Comp Strength		Age Days	Comp Strength		Age Days	Comp Strength	
		KN	PSI		KN	PSI		KN	PSI
1		320	2544		440	3498		520	4134
2	7Days	335	2663	14Days	445	3538	28Days	510	4055
3	30-08-2014	325	2584	03-09-2014	435	3458	24-09-2014	520	4134
Average			2597			3498			4108

Table 7: COMPRESSIVE STRENGTH RESULTS

Table 8: SPECIMEN DETAILS AND MATERIAL PROPERTIES

Beams	f'_c (psi)	Longitudinal tensile bars			Shear steel bars			a/d	d (in)	b (in)
		No	(%)	f_{yl} (ksi)	No	(%)	f_{yt} (ksi)			
N - Series										
N1	4000	3 # 9	1.867	60	-	-	-	2.5	16	10
N2	4000	3 # 9	1.867	60	-	-	-	2.5	16	10
A – Series										
A1	4000	3 # 9	1.867	60	# 2 @ 7.5" c/c	0.13	40	2.5	16	10
A2	4000	3 # 9	1.867	60	# 2 @ 7.5" c/c	0.13	40	2.5	16	10
Z – Series										
Z1	4000	3 # 9	1.867	60	# 3 @ 5" c/c	0.44	40	2.5	16	10
Z2	4000	3 # 9	1.867	60	# 3 @ 5" c/c	0.44	40	2.5	16	10
M – Series										
M1	4000	3 # 9	1.867	60	# 3 @ 7" c/c	0.31	40	3.25	16	10
M2	4000	3 # 9	1.867	60	# 3 @ 7" c/c	0.31	40	3.25	16	10

`

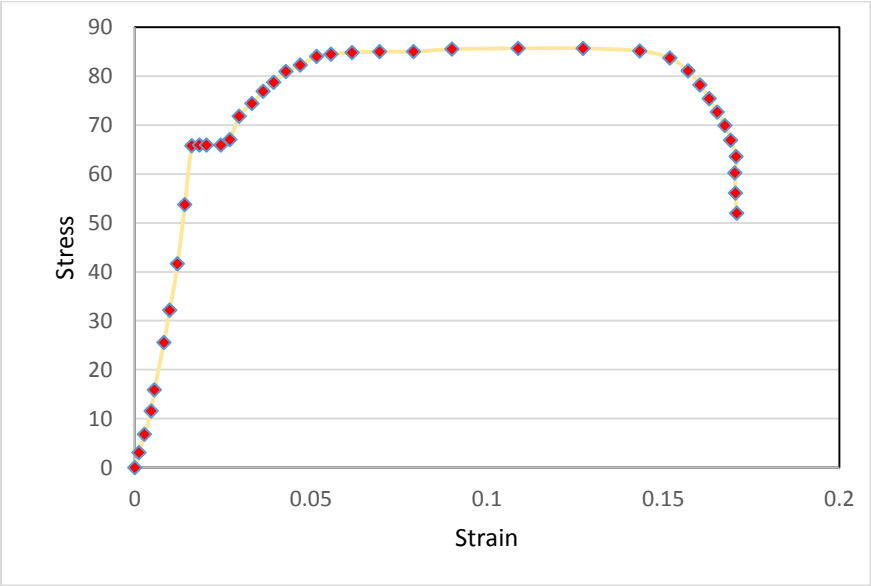

Figure 1: Stress - strain relationship of longitudinal bar

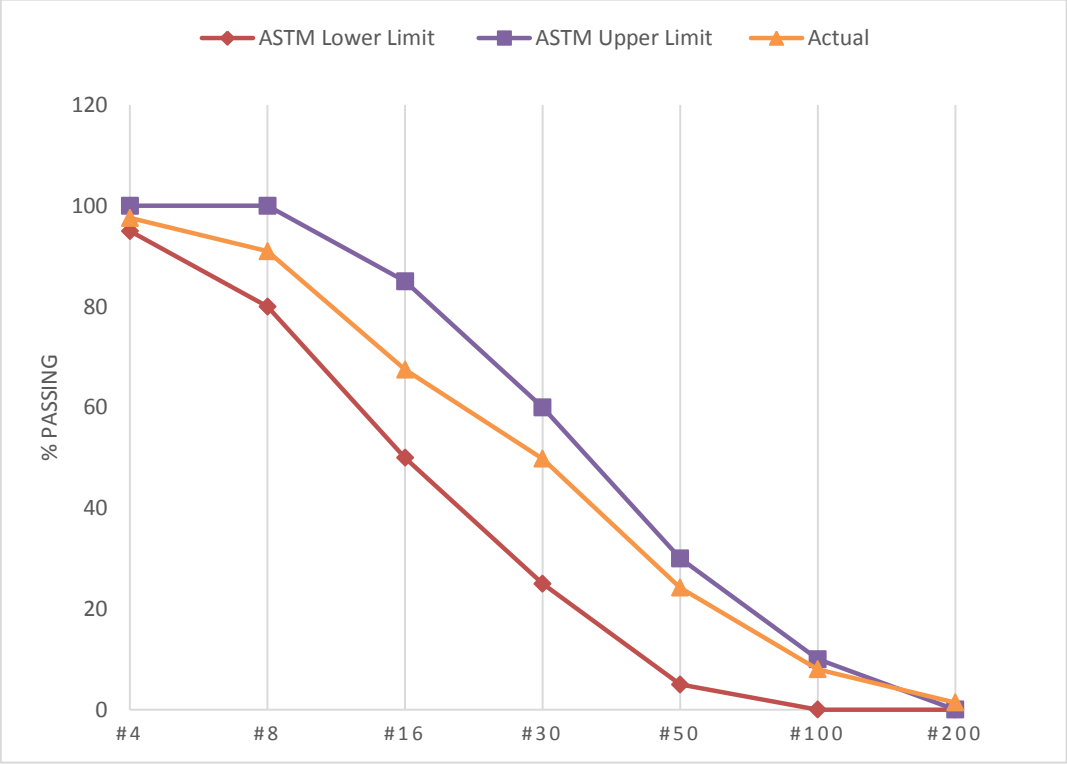

Figure 2 : Gradation of fine aggregate

`

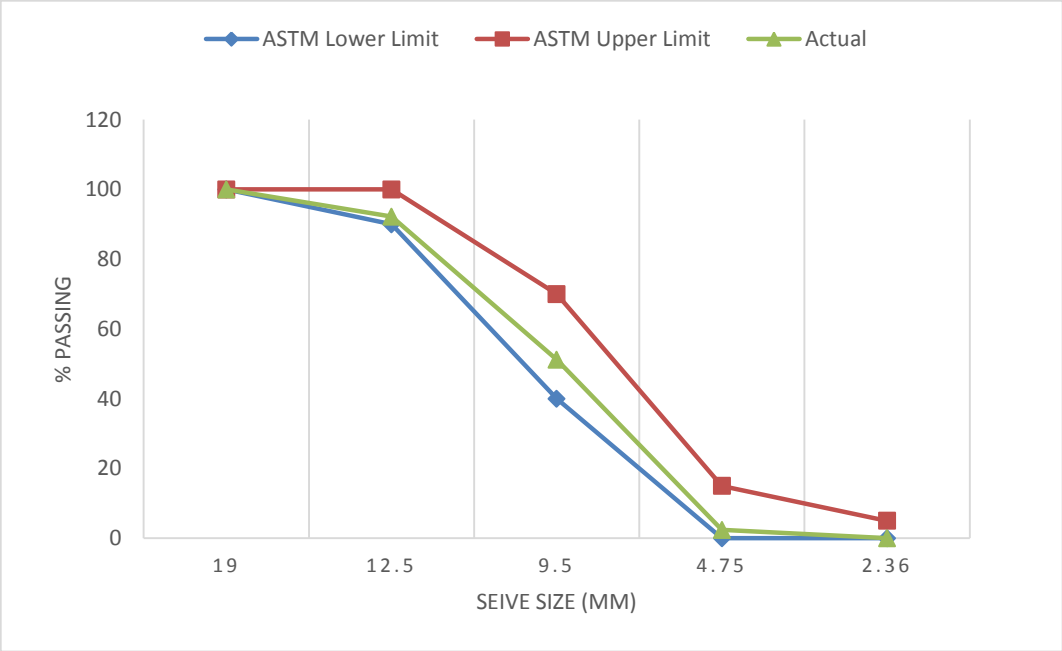

Figure 3: Gradation of coarse aggregate

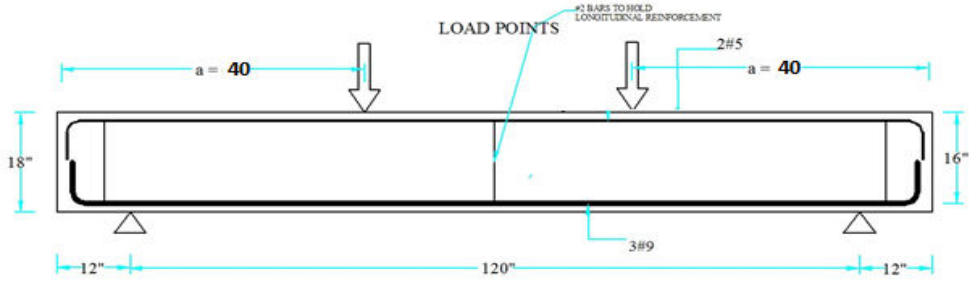

a) No shear reinforcement (N1&N2)

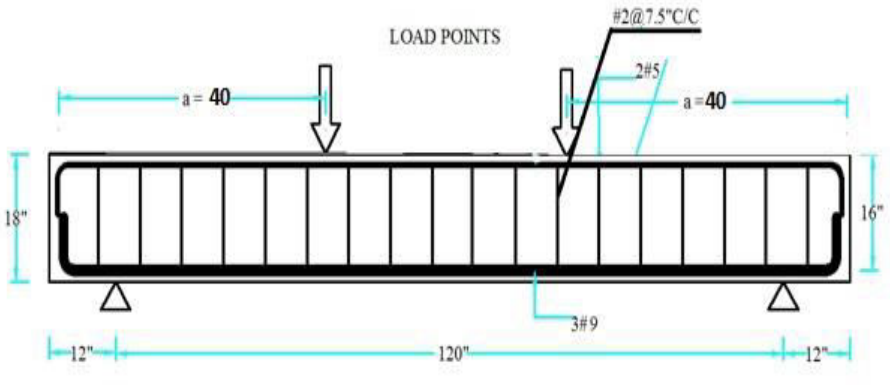

b) **ACI minimum Shear reinforcement (A-1&A-2)**

`

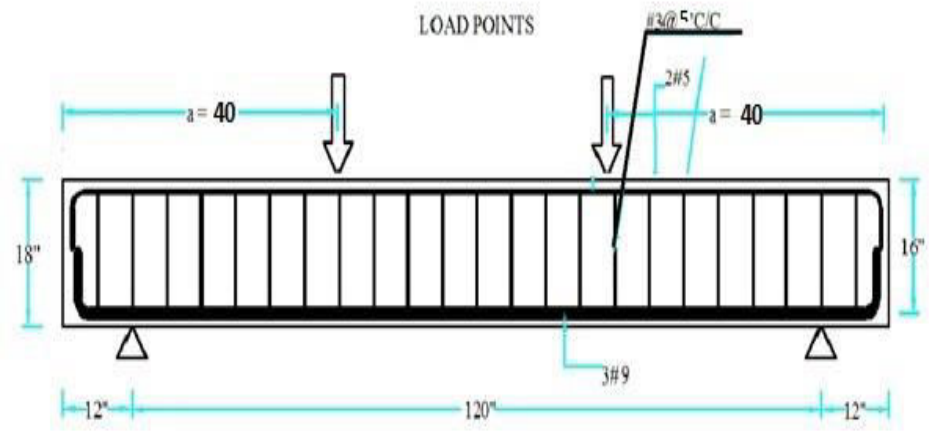

C) Zarari minimum Shear reinforcement (Z-1 & Z-2)

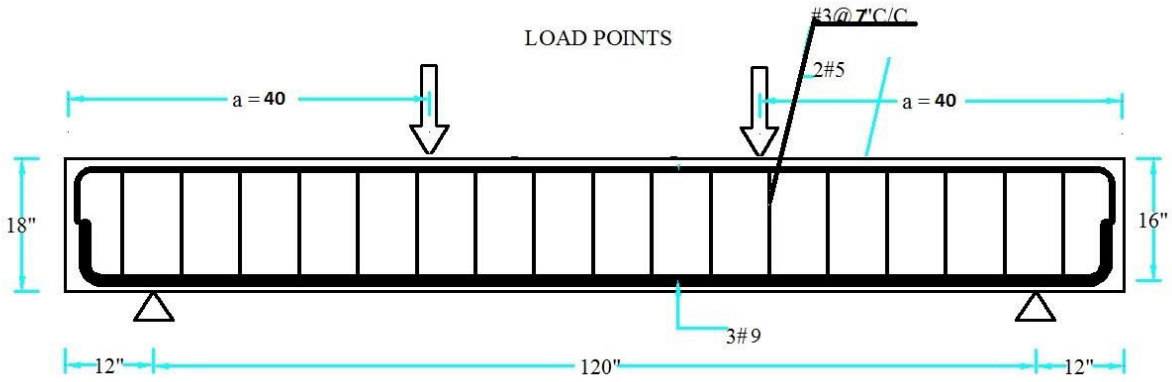

d) Modified Zarari (M-1 &M-2)

`

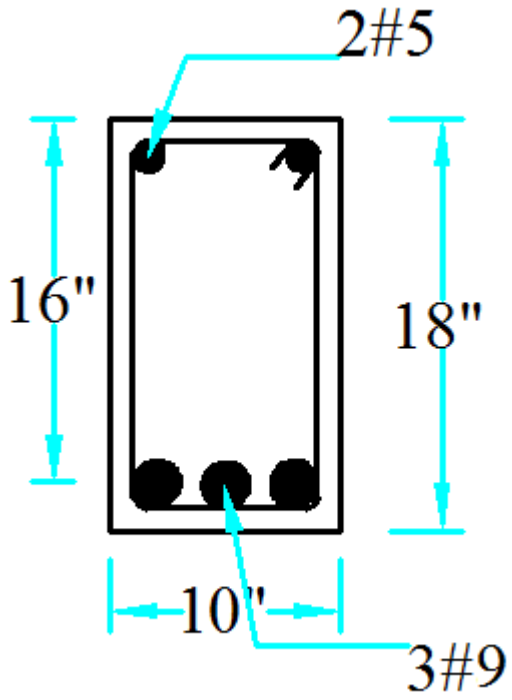

e) Cross- Section of specimen

Figure 4: Dimension and detail of specimens

Figure 5: Specimens transporting to lab with the help of crane

`

Figure 6: Test Set up

Figure 7: Beam Form work

`

Appendix-II

Figure 0- 1: Structural load Analysis and Automation System

`

Table 0-1 : Load Deflection Data of Beam N-1

Load (tons)	Load (kips)	Deflections					
		Mid point		Quarter point		Quarter point	
		mm	Inch	mm	inch	mm	inch
0	0.0	0.0	0.0	0.0	0.0	0.0	0.0
2.5	5.5	0.3	0.0	0.0	0.0	0.7	0.0
5	11.0	0.5	0.0	0.1	0.0	0.9	0.0
7.5	16.5	0.8	0.0	0.3	0.0	1.1	0.0
10	22.0	1.4	0.1	0.7	0.0	1.7	0.1
12.5	27.6	1.8	0.1	0.9	0.0	2.1	0.1
15	33.1	2.5	0.1	1.4	0.1	2.7	0.1
17.5	38.6	3.1	0.1	1.8	0.1	3.3	0.1
20	44.1	4.1	0.2	2.3	0.1	4.1	0.2
23	50.7	4.6	0.2	2.6	0.1	4.6	0.2
25	55.1	6.1	0.2	3.6	0.1	6.2	0.2
27.5	60.6	7.0	0.3	3.6	0.1	7.4	0.3
30	66.1	8.3	0.3	4.6	0.2	8.5	0.3
32.83865	**72.4**	**9.6**	**0.4**	**5.7**	**0.2**	**9.5**	**0.4**
32.5	71.6	9.6	0.4	5.8	0.2	9.5	0.4
30	66.1	11.5	0.5	8.5	0.3	10.3	0.4
26	57.3	12.6	0.5	10.3	0.4	10.6	0.4
25	55.1	12.9	0.5	10.5	0.4	10.7	0.4
24.5	54.0	12.9	0.5	10.5	0.4	10.6	0.4
22.5	49.6	12.5	0.5	10.3	0.4	10.2	0.4
20	44.1	12.0	0.5	10.0	0.4	9.8	0.4
17.5	38.6	11.6	0.5	9.7	0.4	9.4	0.4
15.8	34.8	11.2	0.4	9.5	0.4	9.0	0.4
14.7	32.4	11.0	0.4	9.3	0.4	8.8	0.3
12	26.4	10.3	0.4	8.8	0.3	8.2	0.3
10	22.0	9.9	0.4	8.5	0.3	7.8	0.3
8.5	18.7	9.2	0.4	8.0	0.3	7.2	0.3
6.5	14.3	8.7	0.3	7.6	0.3	6.8	0.3
5.8	12.8	8.3	0.3	7.3	0.3	6.5	0.3
5	11.0	8.1	0.3	7.1	0.3	6.2	0.2
3.5	7.7	7.5	0.3	6.6	0.3	5.8	0.2
3	6.6	7.2	0.3	6.4	0.3	5.5	0.2
2.2	4.8	6.9	0.3	6.1	0.2	5.3	0.2
1.7	3.7	6.7	0.3	5.9	0.2	5.1	0.2
0.87	1.9	6.3	0.2	5.6	0.2	4.8	0.2
0.22	0.5	5.9	0.2	5.2	0.2	4.5	0.2
0.06	0.1	5.5	0.2	4.9	0.2	4.2	0.2

`

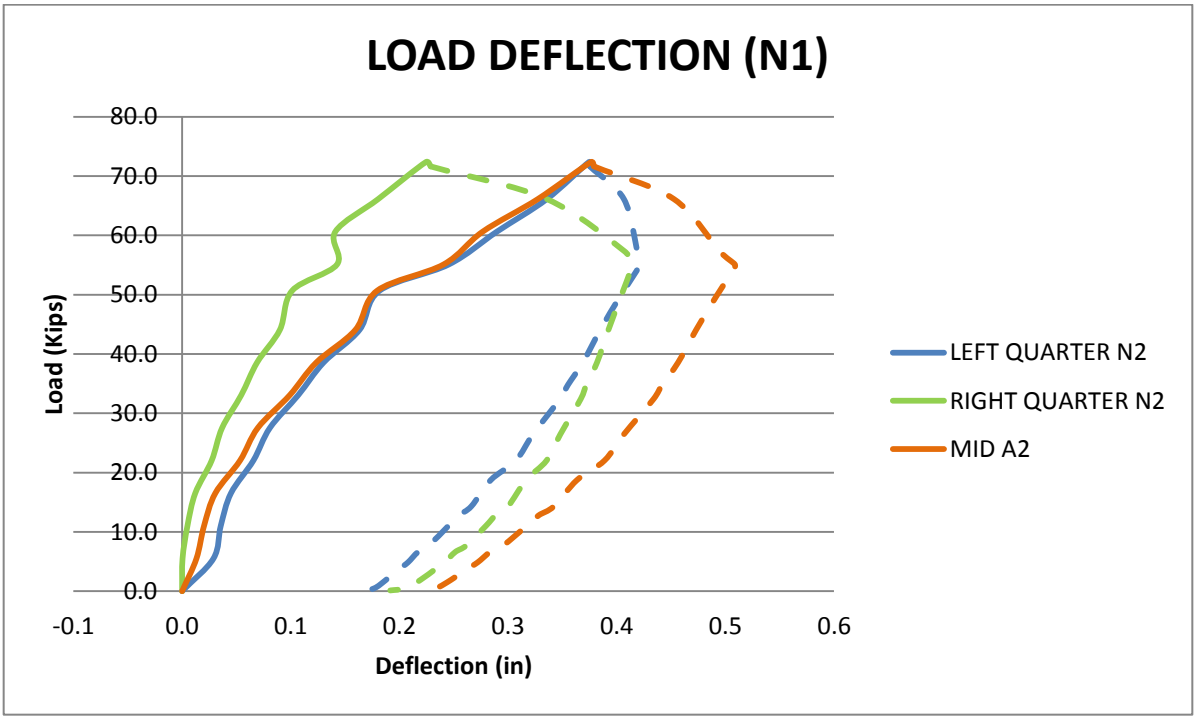

Figure 0 2: Load deflection plot N-1

a) West Ward Face of Beam

b) East Face of Beam

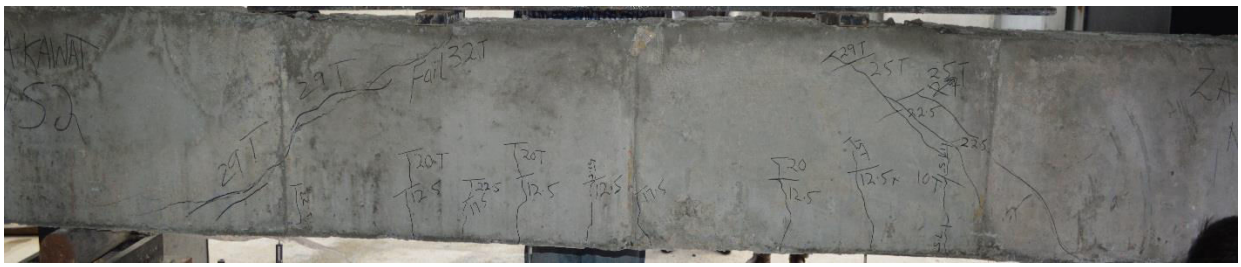

Figure 0 3: Cracking Pattern of N-1

`

Table 0-2 : Load Deflection Data of Beam N-2

Load (tons)	Load (kips	Deflections					
		Mid point		Quarter point		Quarter point	
		mm	inch	mm	inch	mm	inch
0	0	0	0	0	0	0	0
2.5	5.51	0.27	0.01	0.17	0.01	0.27	0.01
5	11.02	0.47	0.02	0.32	0.01	0.51	0.02
7.5	16.53	0.71	0.03	0.45	0.02	0.63	0.02
10	22.04	1.27	0.05	0.72	0.03	1.06	0.04
12.5	27.55	2.09	0.08	1.26	0.05	1.78	0.07
15	33.06	2.90	0.11	1.79	0.07	2.46	0.10
17.5	38.57	3.48	0.14	2.19	0.09	2.96	0.12
20.5	45.182	4.49	0.18	2.93	0.12	3.83	0.15
22.5	49.59	5.87	0.23	3.92	0.15	5.17	0.20
25	55.1	7.01	0.28	4.70	0.19	6.53	0.26
27.5	60.61	9.05	0.36	6.27	0.25	8.73	0.34
30	66.12	9.66	0.38	6.70	0.26	9.32	0.37
31	**68.324**	**10.92**	**0.43**	**7.43**	**0.29**	**10.95**	**0.43**
30	66.12	11.14	0.44	7.53	0.30	11.39	0.45
28.5	62.814	11.17	0.44	7.55	0.30	11.41	0.45
28	61.712	11.09	0.44	7.49	0.29	11.34	0.45
25	55.1	10.62	0.42	7.17	0.28	10.95	0.43
23	50.692	10.21	0.40	6.89	0.27	10.61	0.42
21.5	47.386	9.91	0.39	6.69	0.26	10.36	0.41
19.5	42.978	9.41	0.37	6.35	0.25	9.93	0.39
17.5	38.57	9.02	0.36	6.08	0.24	9.59	0.38
16	35.264	8.66	0.34	5.83	0.23	9.28	0.37
12.5	27.55	7.78	0.31	5.24	0.21	8.48	0.33
11	24.244	7.34	0.29	4.93	0.19	8.05	0.32
9.5	20.938	6.96	0.27	4.67	0.18	7.70	0.30
8	17.632	6.46	0.25	4.35	0.17	7.21	0.28
7.9	17.4116	6.39	0.25	4.30	0.17	7.13	0.28
6.7	14.7668	6.05	0.24	4.08	0.16	6.79	0.27
6	13.224	5.76	0.23	3.89	0.15	6.49	0.26
4.5	9.918	5.40	0.21	3.67	0.14	6.11	0.24
3.5	7.714	4.90	0.19	3.35	0.13	5.56	0.22
2.5	5.51	4.48	0.18	3.09	0.12	5.06	0.20
1.5	3.306	4.09	0.16	2.85	0.11	4.63	0.18
0.5	1.102	3.50	0.14	2.20	0.09	4.46	0.18
0.1	0.2204	3.11	0.12	1.82	0.07	4.20	0.17
0.05	0.1102	2.96	0.12	1.75	0.07	3.97	0.16

`

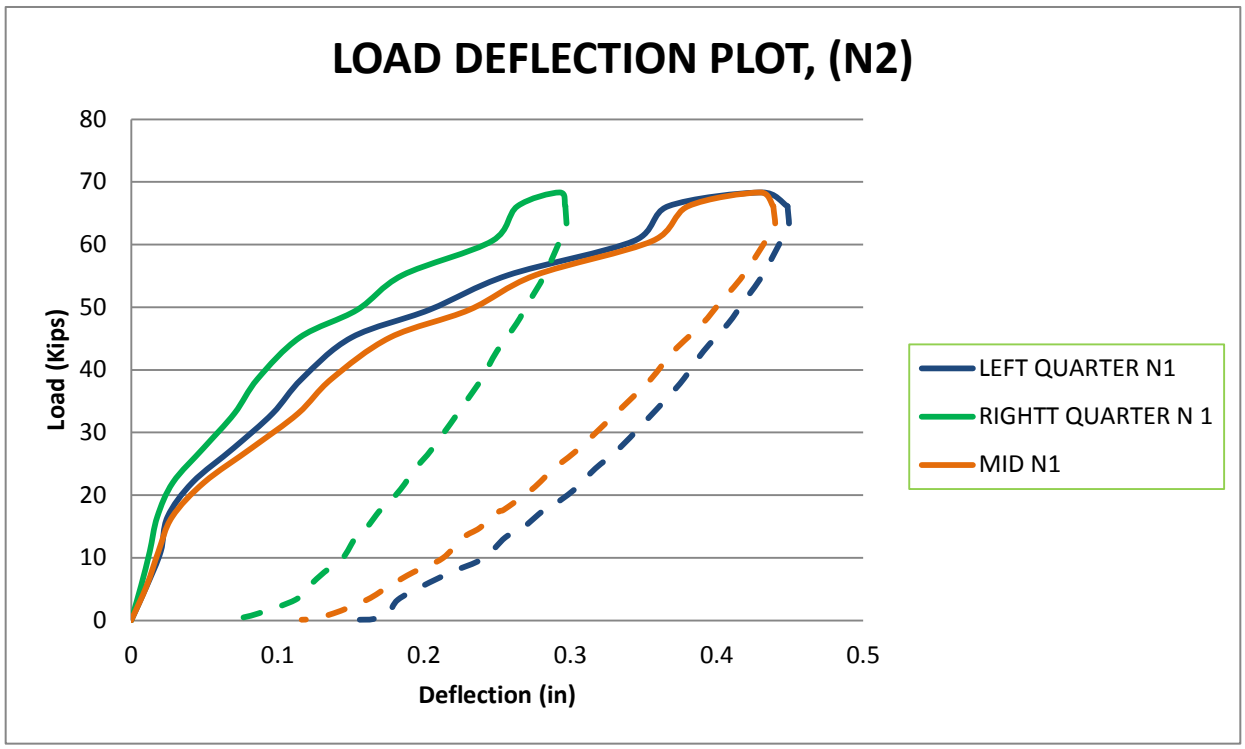

Figure 0 4: Load Deflection Plot N-2

a) West face of beam

b) West Face North Support

Figure 0 5: Cracking Pattern of Beam N-2

`

Table 0-3 : Load Deflection Data of Beam A-1

Load (tons)	Load (kips)	Deflections					
		Mid point		Quarter point		Quarter point	
		mm	inch	mm	inch	mm	inch
0.0	0.0	0.0	0.0	0.0	0.0	0.0	0.0
2.5	5.5	0.6	0.0	0.4	0.0	0.4	0.0
5.0	11.0	1.1	0.0	0.7	0.0	0.8	0.0
7.5	16.5	1.4	0.1	0.9	0.0	1.1	0.0
10.0	22.0	2.1	0.1	1.5	0.1	1.7	0.1
12.5	27.6	2.6	0.1	1.8	0.1	2.0	0.1
15.0	33.1	3.4	0.1	2.3	0.1	2.6	0.1
17.5	38.6	3.9	0.2	2.6	0.1	3.1	0.1
20.0	44.1	4.6	0.2	3.1	0.1	3.7	0.1
22.5	49.6	5.3	0.2	3.3	0.1	4.2	0.2
25.0	55.1	5.6	0.2	3.7	0.1	4.6	0.2
27.5	60.6	6.9	0.3	4.6	0.2	6.0	0.2
30.0	66.1	8.1	0.3	5.8	0.2	6.8	0.3
32.5	71.6	8.9	0.3	6.5	0.3	7.5	0.3
35.0	77.1	9.9	0.4	7.3	0.3	8.7	0.3
37.5	82.7	11.0	0.4	8.1	0.3	9.7	0.4
40.0	88.2	12.4	0.5	9.4	0.4	10.9	0.4
43.0	**94.8**	**13.6**	**0.5**	**10.5**	**0.4**	**11.8**	**0.5**
40.0	88.2	14.4	0.6	11.7	0.5	12.0	0.5
32.0	70.5	21.5	0.8	16.0	0.6	14.2	0.6
30.6	67.4	21.1	0.8	15.3	0.6	14.0	0.6
14.0	30.9	17.9	0.7	11.3	0.4	12.1	0.5
12.0	26.4	17.1	0.7	10.5	0.4	11.5	0.5
10.0	22.0	15.8	0.6	9.8	0.4	11.2	0.4
9.3	20.5	15.5	0.6	9.7	0.4	10.6	0.4
7.0	15.4	14.8	0.6	9.2	0.4	10.2	0.4
5.5	12.1	13.4	0.5	8.1	0.3	9.7	0.4
4.2	9.3	12.7	0.5	7.1	0.3	9.3	0.4
3.2	7.1	11.9	0.5	6.9	0.3	8.8	0.3
2.4	5.3	11.1	0.4	6.4	0.3	8.1	0.3
2.0	4.4	10.7	0.4	6.2	0.2	7.9	0.3
1.8	4.0	10.4	0.4	5.9	0.2	7.3	0.3

`

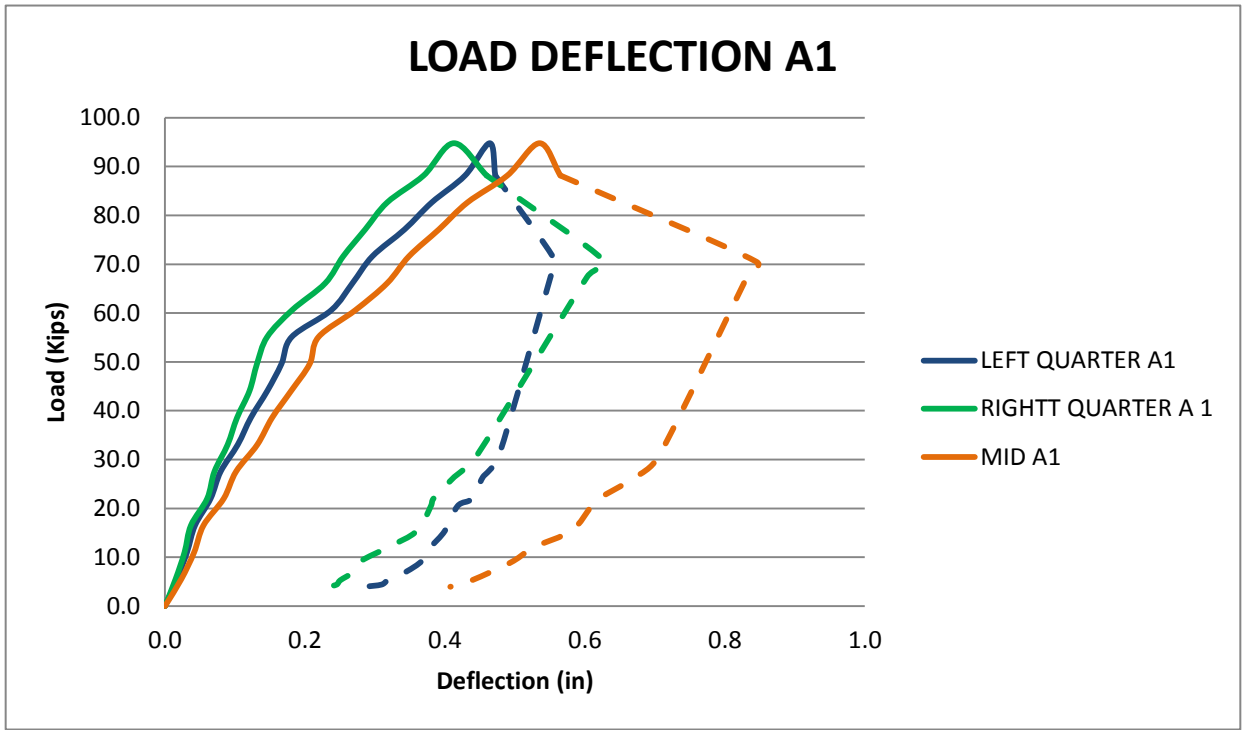

Figure 0 6: Load Deflection Plot A-1

a) West face of beam

b) West Face North Support

Figure 0 7: Cracking Pattern A-1

`

Table 0-4: Load Deflection Data of Beam A-2

Load (tons)	Load (kips)	Deflections					
		Mid point		Quarter point		Quarter point	
		mm	inch	mm	inch	mm	inch
0.0	0.0	0.0	0.0	0.0	0.0	0.0	0.0
2.5	5.5	0.5	0.0	0.0	0.0	0.5	0.0
5.0	11.0	1.0	0.0	0.2	0.0	1.1	0.0
7.5	16.5	1.4	0.1	0.4	0.0	1.5	0.1
10.0	22.0	2.3	0.1	0.8	0.0	2.4	0.1
12.5	27.6	3.0	0.1	1.1	0.0	3.2	0.1
15.0	33.1	3.6	0.1	1.4	0.1	3.8	0.1
17.5	38.6	4.4	0.2	1.7	0.1	4.6	0.2
20.0	44.1	5.0	0.2	2.0	0.1	5.2	0.2
22.0	48.5	5.7	0.2	2.3	0.1	5.8	0.2
25.0	55.1	7.1	0.3	3.3	0.1	7.0	0.3
27.0	59.5	7.4	0.3	3.5	0.1	7.3	0.3
30.0	66.1	8.7	0.3	4.3	0.2	8.6	0.3
32.5	71.6	9.5	0.4	4.7	0.2	9.3	0.4
35.0	77.1	10.8	0.4	5.5	0.2	10.7	0.4
37.5	82.7	11.5	0.5	5.9	0.2	11.5	0.5
40.0	88.2	13.0	0.5	6.9	0.3	13.0	0.5
41.3	**90.9**	**16.2**	**0.6**	**9.5**	**0.4**	**16.5**	**0.7**
40.4	89.0	17.4	0.7	10.0	0.4	18.4	0.7
37.5	82.7	17.8	0.7	10.1	0.4	19.3	0.8
37.0	81.6	17.9	0.7	10.1	0.4	19.5	0.8
36.5	80.4	17.9	0.7	10.2	0.4	19.5	0.8
35.0	77.1	17.8	0.7	10.1	0.4	19.4	0.8
33.5	73.8	17.6	0.7	10.0	0.4	19.2	0.8
26.0	57.3	16.2	0.6	9.3	0.4	17.8	0.7
23.5	51.8	15.7	0.6	9.0	0.4	17.4	0.7
21.0	46.3	15.2	0.6	8.7	0.3	16.9	0.7
20.0	44.1	14.8	0.6	8.5	0.3	16.5	0.6
18.5	40.8	14.5	0.6	8.4	0.3	16.2	0.6
16.5	36.4	14.0	0.6	8.1	0.3	15.7	0.6
14.5	32.0	13.5	0.5	7.7	0.3	15.2	0.6
12.0	26.4	12.7	0.5	7.3	0.3	14.4	0.6
10.0	22.0	12.2	0.5	7.0	0.3	13.9	0.5
8.5	18.7	11.7	0.5	6.7	0.3	13.3	0.5
7.0	15.4	11.2	0.4	6.4	0.3	12.8	0.5
5.5	12.1	10.6	0.4	5.9	0.2	12.1	0.5
4.5	9.9	10.2	0.4	5.7	0.2	11.8	0.5

3.1	6.8	9.7	0.4	5.4	0.2	11.2	0.4
2.0	4.4	9.1	0.4	5.0	0.2	10.6	0.4
1.7	3.6	9.0	0.4	4.8	0.2	10.4	0.4
1.1	2.4	8.7	0.3	4.6	0.2	10.1	0.4
0.1	0.1	7.8	0.3	4.0	0.2	9.2	0.4

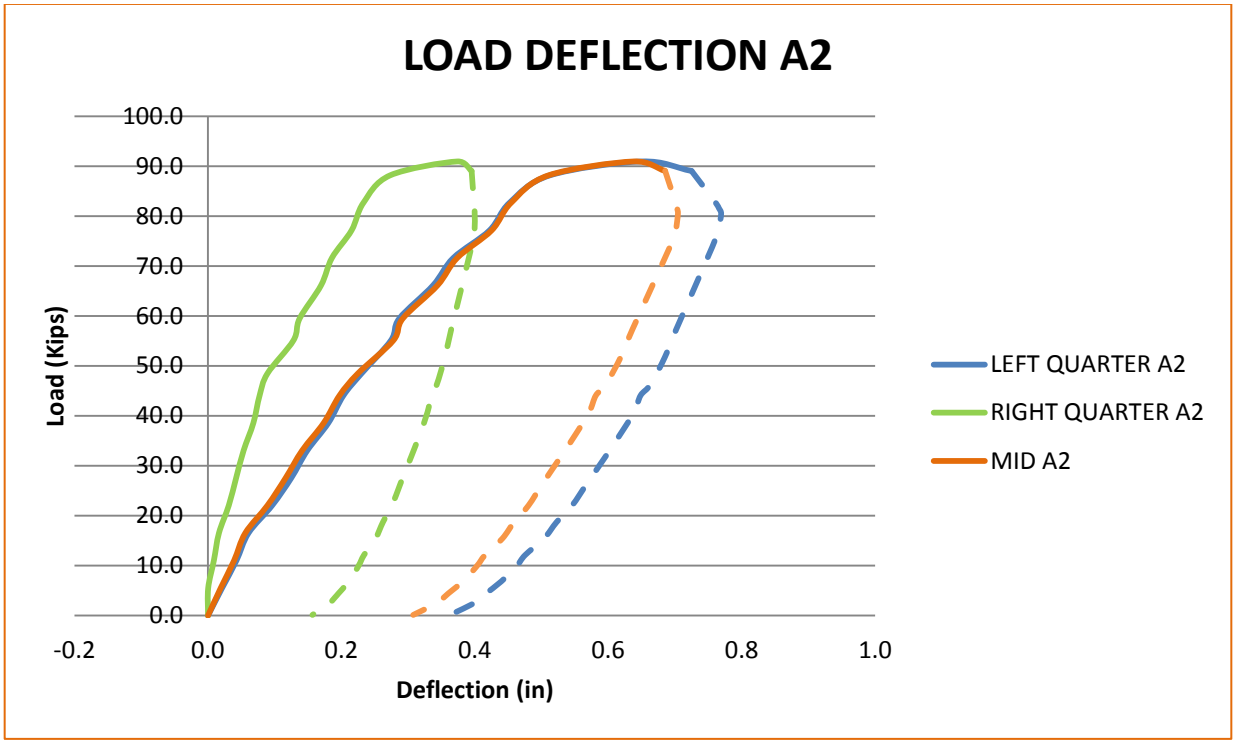

Figure 0 8 :Load Deflection Plot A-2

a) West face of beam

b West face North Support

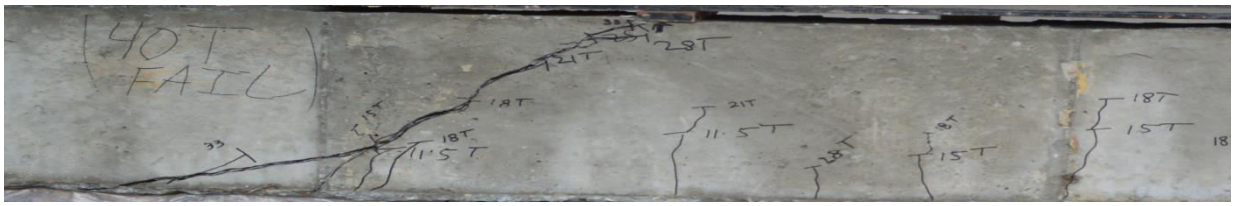

Figure 0 9: Cracking Pattern A-2

`

Table 0-5 : Load Deflection Data of Beam Z-1

Load (tons)	Load (kips)	Deflections					
		Mid point		Quarter point		Quarter point	
		mm	inch	mm	inch	mm	inch
0.0	0.0	0.0	0.0	0.0	0.0	0.0	0.0
2.5	5.5	0.5	0.0	0.4	0.0	0.4	0.0
5.0	11.0	1.1	0.0	0.9	0.0	0.8	0.0
7.5	16.5	1.8	0.1	1.4	0.1	1.3	0.1
10.0	22.0	2.2	0.1	1.7	0.1	1.7	0.1
12.5	27.6	2.9	0.1	2.2	0.1	2.3	0.1
15.0	33.1	3.6	0.1	2.7	0.1	2.9	0.1
17.5	38.6	4.5	0.2	3.0	0.1	2.7	0.1
20.0	44.1	5.1	0.2	3.4	0.1	3.2	0.1
23.0	50.7	5.8	0.2	3.9	0.2	3.9	0.2
25.0	55.1	6.4	0.3	4.4	0.2	4.4	0.2
27.5	60.6	7.4	0.3	5.1	0.2	5.4	0.2
30.0	66.1	8.2	0.3	5.7	0.2	6.1	0.2
32.5	71.6	8.8	0.3	6.1	0.2	6.7	0.3
35.0	77.1	9.3	0.4	6.5	0.3	7.1	0.3
37.5	82.7	10.1	0.4	7.1	0.3	7.9	0.3
40.0	88.2	10.8	0.4	7.6	0.3	8.6	0.3
42.5	93.7	11.6	0.5	8.2	0.3	9.4	0.4
45.0	99.2	11.9	0.5	8.4	0.3	9.7	0.4
47.5	104.7	12.7	0.5	9.0	0.4	10.5	0.4
50.0	110.2	13.5	0.5	9.6	0.4	11.2	0.4
52.5	115.7	14.2	0.6	10.2	0.4	11.9	0.5
55.0	121.2	15.4	0.6	11.1	0.4	13.1	0.5
57.5	126.7	15.8	0.6	11.4	0.4	13.5	0.5
60.0	132.2	16.6	0.7	12.0	0.5	14.3	0.6
62.5	137.8	18.3	0.7	13.3	0.5	15.9	0.6
65.0	143.3	19.0	0.7	13.9	0.5	16.6	0.6
67.1	147.9	19.4	0.8	14.2	0.6	17.0	0.7
67.5	**148.8**	**21.0**	**0.8**	**15.3**	**0.6**	**18.8**	**0.7**
65.0	143.3	21.4	0.8	15.5	0.6	19.4	0.8
55.5	122.3	23.3	0.9	16.0	0.6	20.9	0.8
36.5	80.4	26.7	1.0	17.0	0.7	23.9	0.9
35.5	78.2	26.6	1.0	16.9	0.7	23.8	0.9
32.0	70.5	26.0	1.0	16.5	0.6	23.1	0.9
28.5	62.8	25.3	1.0	16.0	0.6	22.0	0.9
25.3	55.8	24.5	1.0	15.5	0.6	21.5	0.8
20.7	45.6	23.3	0.9	14.7	0.6	20.1	0.8

`

18.0	39.7		22.6	0.9	14.2	0.6	19.3	0.8
15.5	34.2		21.9	0.9	13.8	0.5	18.5	0.7
13.2	29.0		21.2	0.8	13.3	0.5	17.2	0.7
11.0	24.2		20.6	0.8	12.8	0.5	16.8	0.7
9.0	19.8		19.9	0.8	12.4	0.5	16.3	0.6
7.5	16.5		19.2	0.8	11.9	0.5	16.0	0.6
5.3	11.8		18.4	0.7	11.4	0.4	15.4	0.6
4.0	8.8		17.8	0.7	11.1	0.4	15.1	0.6
2.8	6.2		17.2	0.7	10.7	0.4	14.7	0.6
2.3	5.0		16.9	0.7	10.5	0.4	14.3	0.6
2.0	4.4		16.8	0.7	10.4	0.4	14.3	0.6
1.4	3.1		16.5	0.6	10.2	0.4	14.1	0.6
0.6	1.4		16.1	0.6	10.0	0.4	13.9	0.5
0.2	0.4		15.8	0.6	9.8	0.4	13.6	0.5
0.1	0.2		15.4	0.6	9.5	0.4	13.5	0.5

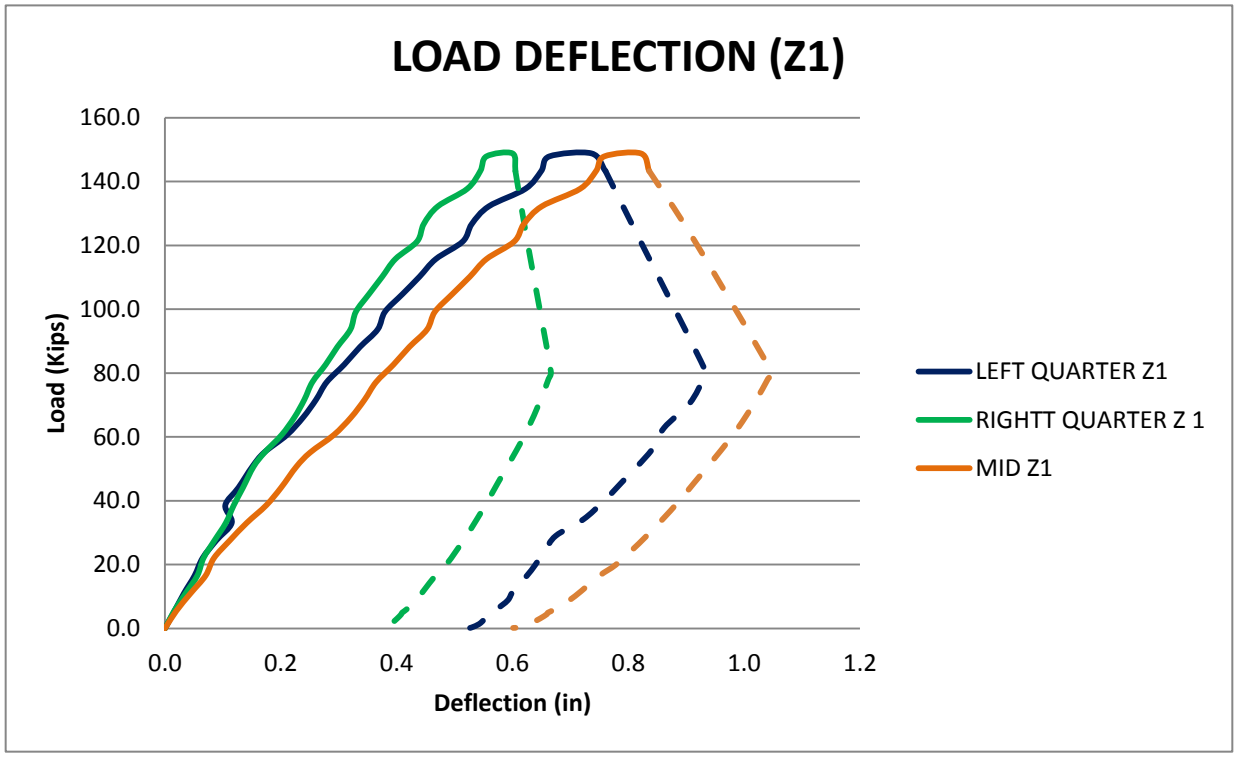

Figure 0 10 :Load Deflection Plot Z-1

a) West Face of Beam

b) East face of beam

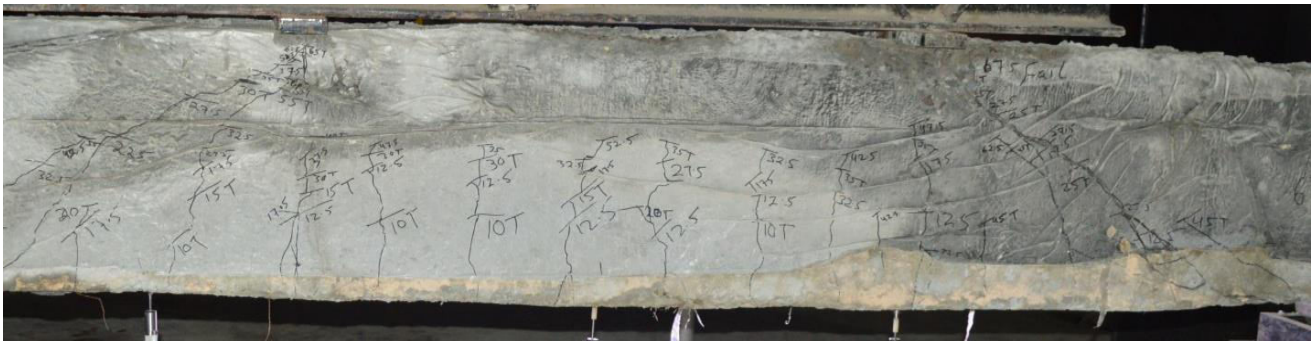

c) West face North Support

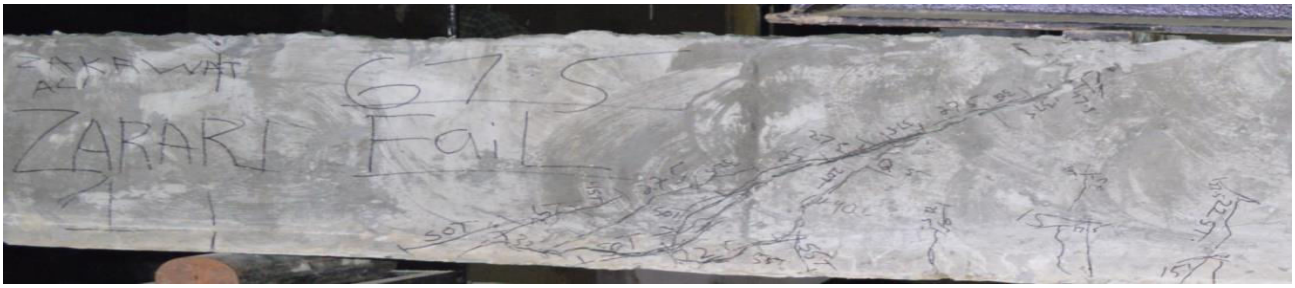

d) West Face South Support

Figure 0 11: Cracking Pattern Z-1

`

Table 0-6 : Load Deflection Data of Beam Z-2

Load (tons)	Load (kips)	Deflections					
		Mid point		Quarter point		Quarter point	
		mm	inch	mm	inch	mm	inch
0	0.0	0	0.0	0	0.0	0	0.0
2.5	5.5	0.147171	0.0	0.0739	0.0	0.123512	0.0
5	11.0	0.541537	0.0	0.227375	0.0	0.393022	0.0
7.5	16.5	0.882069	0.0	0.459483	0.0	0.634203	0.0
10	22.0	1.523202	0.1	0.797936	0.0	1.07377	0.0
12.5	27.6	2.164289	0.1	1.105093	0.0	1.419483	0.1
15	33.1	3.135582	0.1	1.612944	0.1	1.968402	0.1
17.5	38.6	3.717389	0.1	2.079998	0.1	2.391414	0.1
20	44.1	5.126343	0.2	3.101342	0.1	2.904089	0.1
22.5	49.6	5.540826	0.2	3.497988	0.1	3.455016	0.1
25	55.1	6.679538	0.3	4.653504	0.2	4.284573	0.2
27.5	60.6	7.285255	0.3	5.143535	0.2	4.762257	0.2
30	66.1	8.354079	0.3	6.09466	0.2	5.583119	0.2
32.5	71.6	8.668834	0.3	6.329964	0.2	5.81804	0.2
35	77.1	9.57513	0.4	7.05054	0.3	6.491424	0.3
37.5	82.7	10.49426	0.4	7.85559	0.3	7.148671	0.3
40	88.2	11.05255	0.4	8.256274	0.3	7.564052	0.3
42.5	93.7	11.94522	0.5	8.937895	0.3	8.205044	0.3
45	99.2	12.44284	0.5	9.323905	0.4	8.565516	0.3
47.5	104.7	13.24681	0.5	9.988909	0.4	9.143945	0.4
50	110.2	14.1566	0.6	10.74854	0.4	9.795049	0.4
52.5	115.7	14.69912	0.6	11.16225	0.4	10.19933	0.4
55	121.2	15.87882	0.6	12.11014	0.5	11.02761	0.4
57.5	126.7	16.55589	0.6	12.70719	0.5	11.5	0.5
59.85435	**131.9**	**17.87667**	**0.7**	**14.05798**	**0.6**	**12.32885**	**0.5**
58.5	128.9	17.9309	0.7	14.1533	0.6	12.34536	0.5
55	121.2	18.69704	0.7	15.51498	0.6	12.56996	0.5
50.7	111.7	19.59575	0.8	17.16536	0.7	12.84497	0.5
50	110.2	19.7211	0.8	17.40876	0.7	12.89043	0.5
47.6	104.9	19.90337	0.8	17.8933	0.7	12.85723	0.5
45	99.2	19.53914	0.8	17.63201	0.7	12.59103	0.5
42.3	93.2	19.12577	0.7	17.33662	0.7	12.29135	0.5
40.5	89.3	18.83311	0.7	17.12794	0.7	12.0793	0.5
38.6	85.1	18.50013	0.7	16.88998	0.7	11.83845	0.5
35.6	78.5	17.96093	0.7	16.50532	0.6	11.45031	0.4
33	72.7	17.47677	0.7	16.15675	0.6	11.09728	0.4
32	70.5	17.31608	0.7	16.04444	0.6	10.98146	0.4
29.5	65.0	16.81624	0.7	15.68515	0.6	10.61582	0.4
29	63.9	16.65872	0.7	15.5686	0.6	10.50387	0.4

`

25	55.1	15.89877	0.6	15.01794	0.6	9.949993	0.4
22.5	49.6	15.33109	0.6	14.60705	0.6	9.537329	0.4
20	44.1	14.70411	0.6	14.14464	0.6	9.081452	0.4
18.7	41.2	14.42515	0.6	13.93525	0.5	8.88183	0.3
16.1	35.5	13.84908	0.5	13.50793	0.5	8.46515	0.3
14.9	32.8	13.48684	0.5	13.22901	0.5	8.202161	0.3
13.4	29.5	13.12573	0.5	12.95591	0.5	7.943047	0.3
11	24.2	12.49069	0.5	12.46287	0.5	7.485328	0.3
9.9	21.8	12.09929	0.5	12.14502	0.5	7.200484	0.3
8.5	18.7	11.78056	0.5	11.89255	0.5	6.96769	0.3
6.5	14.3	11.17031	0.4	11.38478	0.4	6.523131	0.3
4.9	10.8	10.56863	0.4	10.86417	0.4	6.082068	0.2
3.9	8.6	10.30165	0.4	10.63589	0.4	5.889463	0.2
2.58	5.7	9.846128	0.4	10.22755	0.4	5.558075	0.2
2	4.4	9.623636	0.4	10.02477	0.4	5.392948	0.2
1.85	4.1	9.528231	0.4	9.934692	0.4	5.319587	0.2
1.15	2.5	9.30562	0.4	9.741297	0.4	5.169629	0.2
0.09	0.2	8.676725	0.3	9.206868	0.4	4.742718	0.2

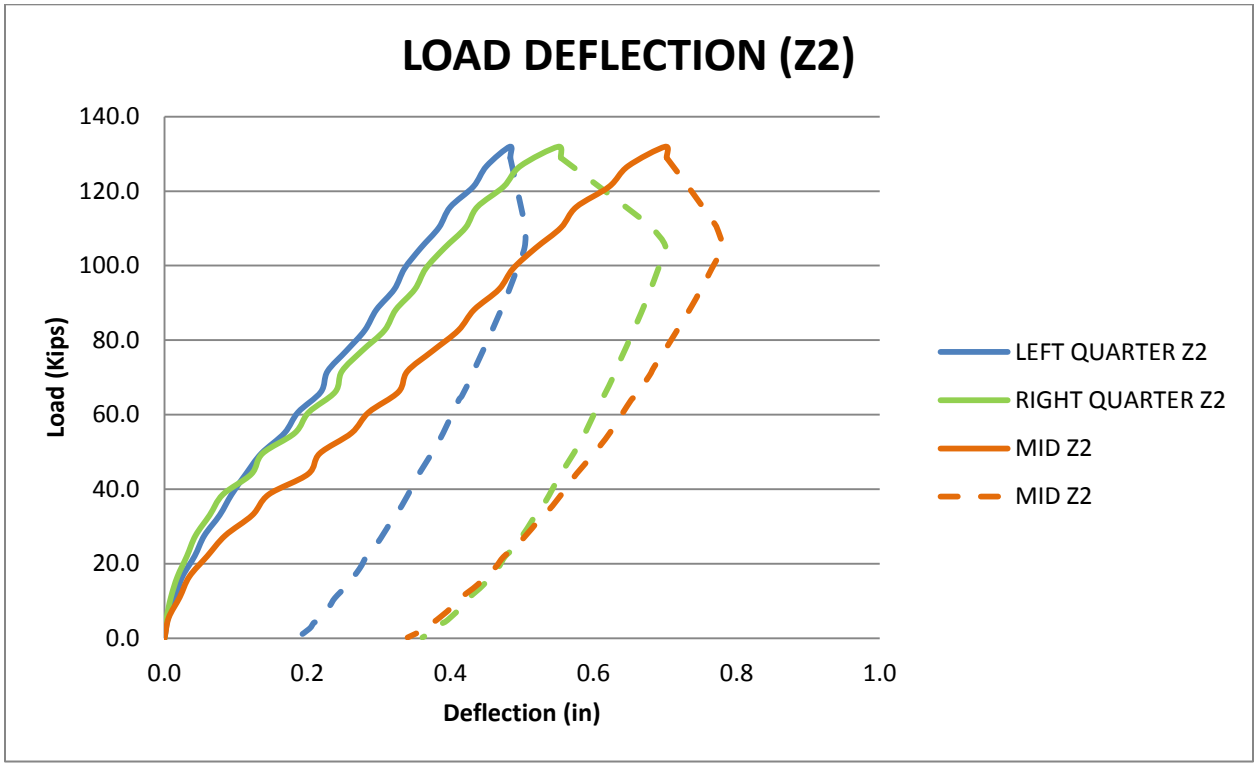

Figure 0 12 : Load Deflection Plot Z-2

a) West face of beam

b) East face of beam

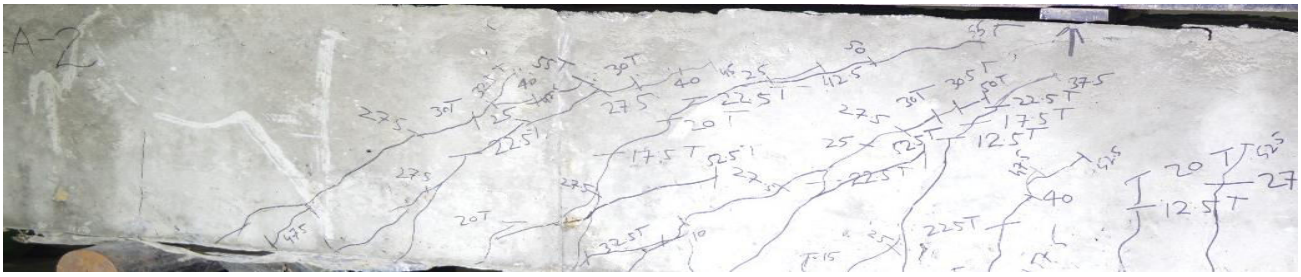

Figure 0 13: Cracking Pattern Z-2

Table 0-7: Load Deflection Data of Beam MZ-1

Load (tons)	Load (kips)	Deflections					
		Mid point		Quarter point		Quarter point	
		mm	inch	mm	inch	mm	inch
0.0	0.0	0.0	0.0	0.0	0.0	0.0	0.0
2.5	5.5	0.4	0.0	0.3	0.0	0.4	0.0
5.0	11.0	0.8	0.0	0.5	0.0	0.9	0.0
7.5	16.5	1.4	0.1	1.0	0.0	1.3	0.1
10.0	22.0	1.9	0.1	1.1	0.0	1.8	0.1
12.5	27.6	2.4	0.1	1.5	0.1	2.2	0.1
15.0	33.1	2.9	0.1	1.9	0.1	2.5	0.1
17.5	38.6	3.6	0.1	2.4	0.1	2.9	0.1
20.0	44.1	4.4	0.2	3.2	0.1	3.4	0.1
22.5	49.6	4.9	0.2	3.8	0.1	3.9	0.2
25.0	55.1	5.7	0.2	4.5	0.2	4.5	0.2
27.5	60.6	6.6	0.3	5.2	0.2	5.1	0.2
30.0	66.1	7.4	0.3	5.8	0.2	5.8	0.2
32.5	71.6	8.0	0.3	6.4	0.3	6.3	0.2
35.0	77.1	8.7	0.3	6.9	0.3	6.9	0.3
37.5	82.7	9.6	0.4	7.7	0.3	7.6	0.3
40.0	88.2	10.6	0.4	8.5	0.3	8.3	0.3

42.5	93.7	11.3	0.4	9.1	0.4	8.8	0.3
45.0	99.2	12.2	0.5	9.8	0.4	9.5	0.4
47.5	104.7	13.1	0.5	10.6	0.4	10.2	0.4
50.0	110.2	14.2	0.6	11.7	0.5	11.0	0.4
52.5	115.7	15.1	0.6	12.5	0.5	11.7	0.5
55.0	121.2	17.6	0.7	15.0	0.6	14.2	0.6
57.6	**126.9**	**19.2**	**0.8**	**16.5**	**0.6**	**15.8**	**0.6**
52.5	115.7	19.8	0.8	17.2	0.7	16.4	0.6
45.3	99.8	20.2	0.8	17.5	0.7	16.8	0.7
43.9	96.8	20.7	0.8	18.0	0.7	17.3	0.7
39.6	87.3	20.9	0.8	18.3	0.7	17.5	0.7
37.1	81.8	20.1	0.8	17.4	0.7	16.7	0.7
30.9	68.1	18.4	0.7	15.8	0.6	15.1	0.6
22.7	50.0	16.8	0.7	14.7	0.6	13.4	0.5
20.5	45.2	16.2	0.6	13.9	0.5	12.9	0.5
18.9	41.7	15.6	0.6	12.9	0.5	12.1	0.5
15.8	34.8	14.2	0.6	11.6	0.5	10.8	0.4
12.1	26.7	13.1	0.5	10.5	0.4	9.7	0.4
10.8	23.8	11.4	0.4	8.7	0.3	8.0	0.3
8.5	18.7	11.0	0.4	8.3	0.3	7.6	0.3
6.1	13.4	10.3	0.4	7.7	0.3	6.9	0.3
0.1	0.1	7.1	0.3	4.5	0.2	3.7	0.1

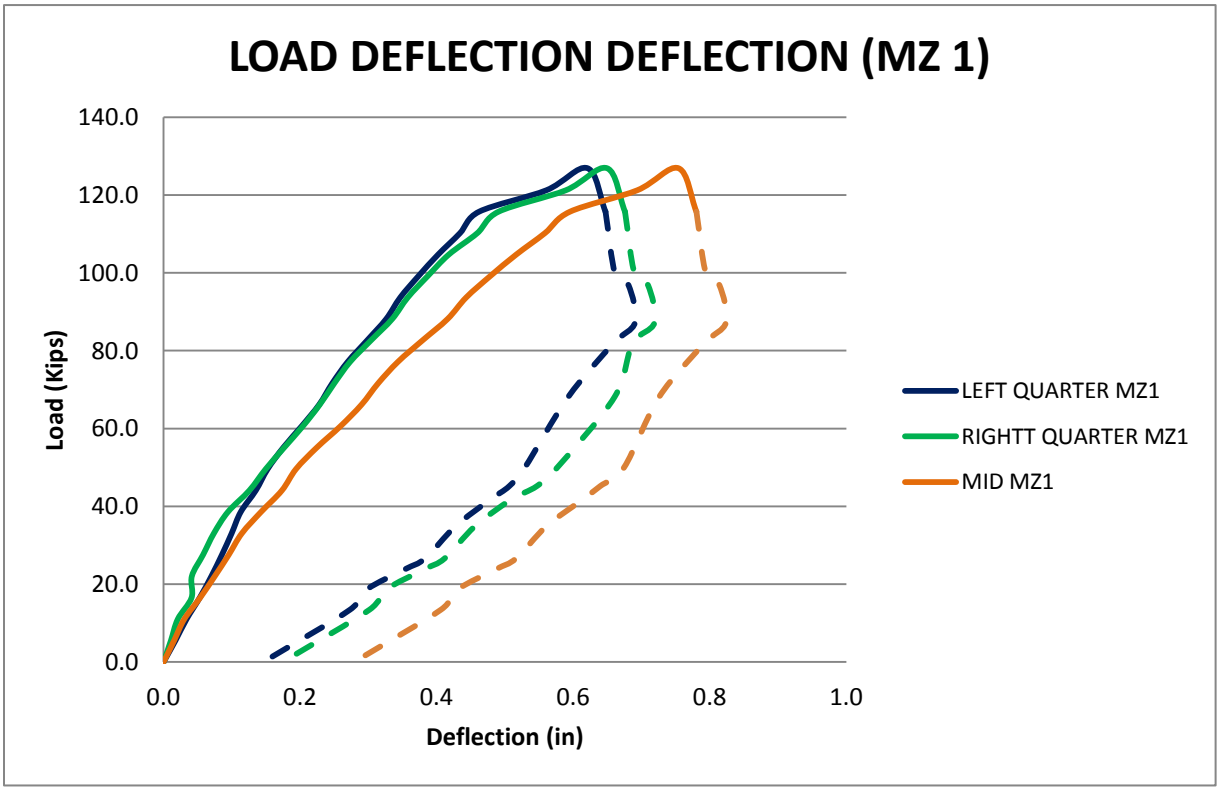

Figure 0 14: Load deflection plot of Beam MZ-1

`

a) East face of beam

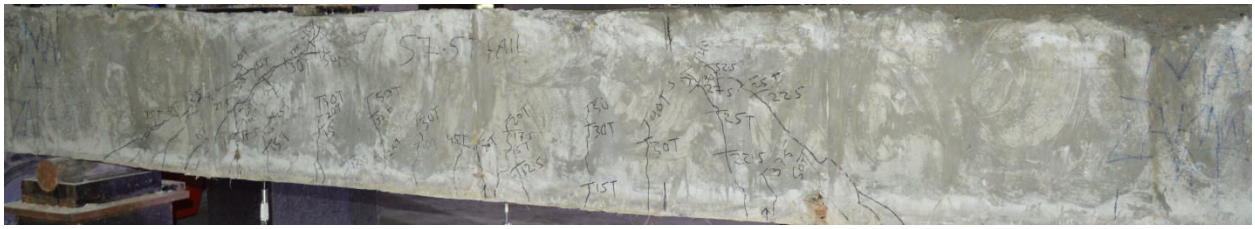

b East Face South Support

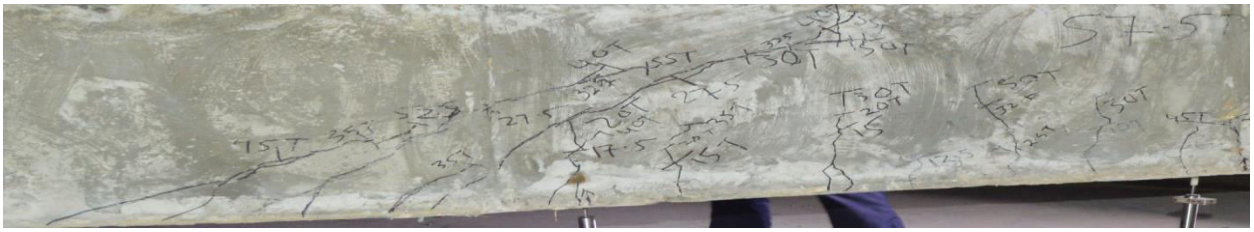

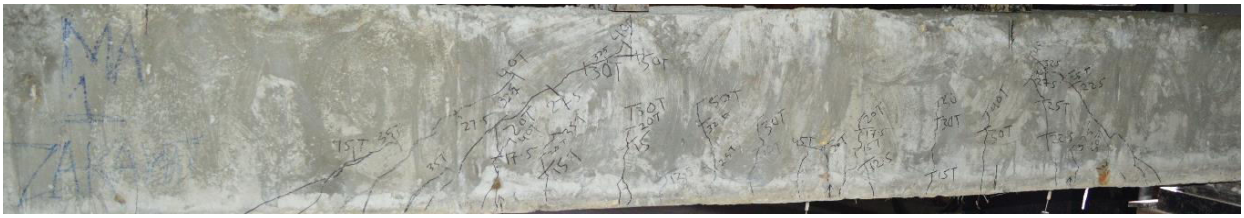

c West face North Support

Figure 0 15: Cracking Pattern of MZ-1

`

Table 0-8 : Load deflection Data of Beam MZ-2

Load (tons)	Load (kips)	Deflections					
		Mid point		Quarter point		Quarter point	
		mm	inch	mm	inch	mm	inch
0.0	0.0	0.0	0.0	0.0	0.0	0.0	0.0
2.5	5.5	0.5	0.0	0.2	0.0	0.7	0.0
5.0	11.0	1.0	0.0	0.5	0.0	1.3	0.1
7.5	16.5	1.5	0.1	0.9	0.0	1.8	0.1
10.0	22.0	2.1	0.1	0.4	0.0	2.3	0.1
12.5	27.6	2.7	0.1	0.8	0.0	2.7	0.1
15.0	33.1	3.2	0.1	1.1	0.0	3.1	0.1
17.5	38.6	4.1	0.2	1.6	0.1	3.8	0.1
20.0	44.1	4.9	0.2	2.5	0.1	4.4	0.2
23.0	50.7	5.5	0.2	3.2	0.1	4.9	0.2
25.0	55.1	6.2	0.2	3.7	0.1	5.4	0.2
27.5	60.6	7.0	0.3	4.2	0.2	6.1	0.2
30.0	66.1	8.0	0.3	4.9	0.2	6.8	0.3
32.5	71.6	8.5	0.3	5.2	0.2	7.3	0.3
35.0	77.1	9.5	0.4	5.9	0.2	8.0	0.3
37.5	82.7	10.4	0.4	6.5	0.3	8.7	0.3
40.0	88.2	11.2	0.4	7.1	0.3	9.4	0.4
42.5	93.7	11.9	0.5	7.6	0.3	9.9	0.4
45.0	99.2	13.0	0.5	8.3	0.3	10.7	0.4
47.5	104.7	14.2	0.6	9.2	0.4	11.7	0.5
50.0	110.2	15.3	0.6	10.2	0.4	12.4	0.5
52.7	**116.2**	**16.2**	**0.6**	**10.9**	**0.4**	**13.1**	**0.5**
52.0	114.6	16.3	0.6	11.0	0.4	13.2	0.5
50.0	110.2	16.6	0.7	11.5	0.5	13.3	0.5
47.0	103.6	19.2	0.8	15.3	0.6	14.5	0.6
45.5	100.3	20.2	0.8	16.9	0.7	15.0	0.6
44.0	97.0	22.2	0.9	20.0	0.8	15.9	0.6
43.0	94.8	26.7	1.1	26.5	1.0	18.2	0.7
37.2	82.0	25.9	1.0	25.9	1.0	17.6	0.7
33.0	72.7	25.0	1.0	25.4	1.0	17.0	0.7
30.0	66.1	24.4	1.0	24.9	1.0	16.6	0.7
25.0	55.1	23.1	0.9	24.1	0.9	15.7	0.6
22.5	49.6	22.6	0.9	23.7	0.9	15.3	0.6
20.0	44.1	21.9	0.9	23.2	0.9	14.8	0.6
17.5	38.6	21.2	0.8	22.1	0.9	14.4	0.6
15.0	33.1	20.5	0.8	21.7	0.9	13.9	0.5
12.8	28.2	19.8	0.8	21.4	0.8	13.3	0.5
10.7	23.6	19.1	0.8	21.0	0.8	12.8	0.5

`

8.8	19.4	18.4	0.7	20.5	0.8	12.4	0.5
7.0	15.4	17.8	0.7	20.0	0.8	11.9	0.5
5.3	11.7	17.1	0.7	19.5	0.8	11.4	0.5
4.0	8.8	16.6	0.7	19.0	0.7	11.0	0.4
2.7	6.0	16.0	0.6	18.6	0.7	10.7	0.4
2.3	5.1	15.8	0.6	18.3	0.7	10.5	0.4
1.9	4.2	15.6	0.6	18.2	0.7	10.4	0.4
1.7	3.7	15.5	0.6	18.1	0.7	10.3	0.4
0.8	1.8	15.1	0.6	17.7	0.7	10.0	0.4
0.1	0.2	14.5	0.6	17.2	0.7	9.6	0.4

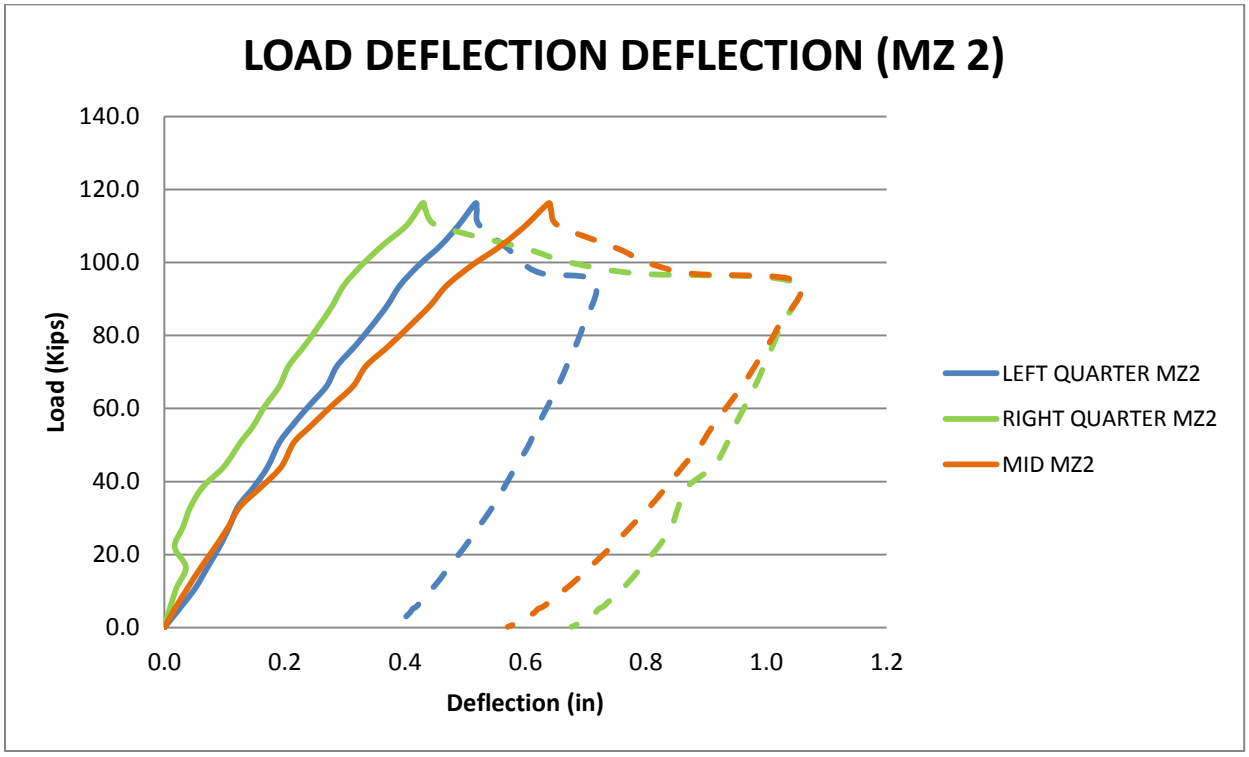

Figure 0 16 :Load deflection Plot MZ-2

a) East face of beam

b)West Face North Support

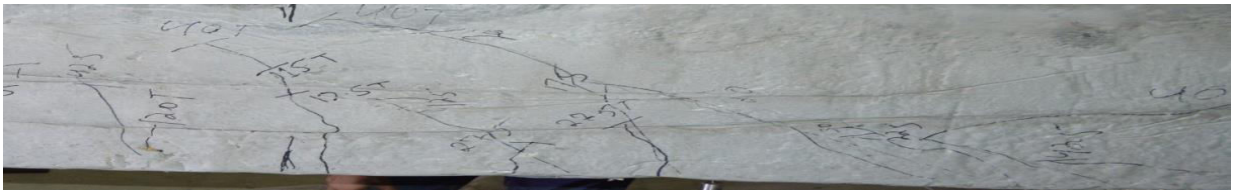

`

Figure 0 17 Cracking pattern of MZ-2

Appendix III

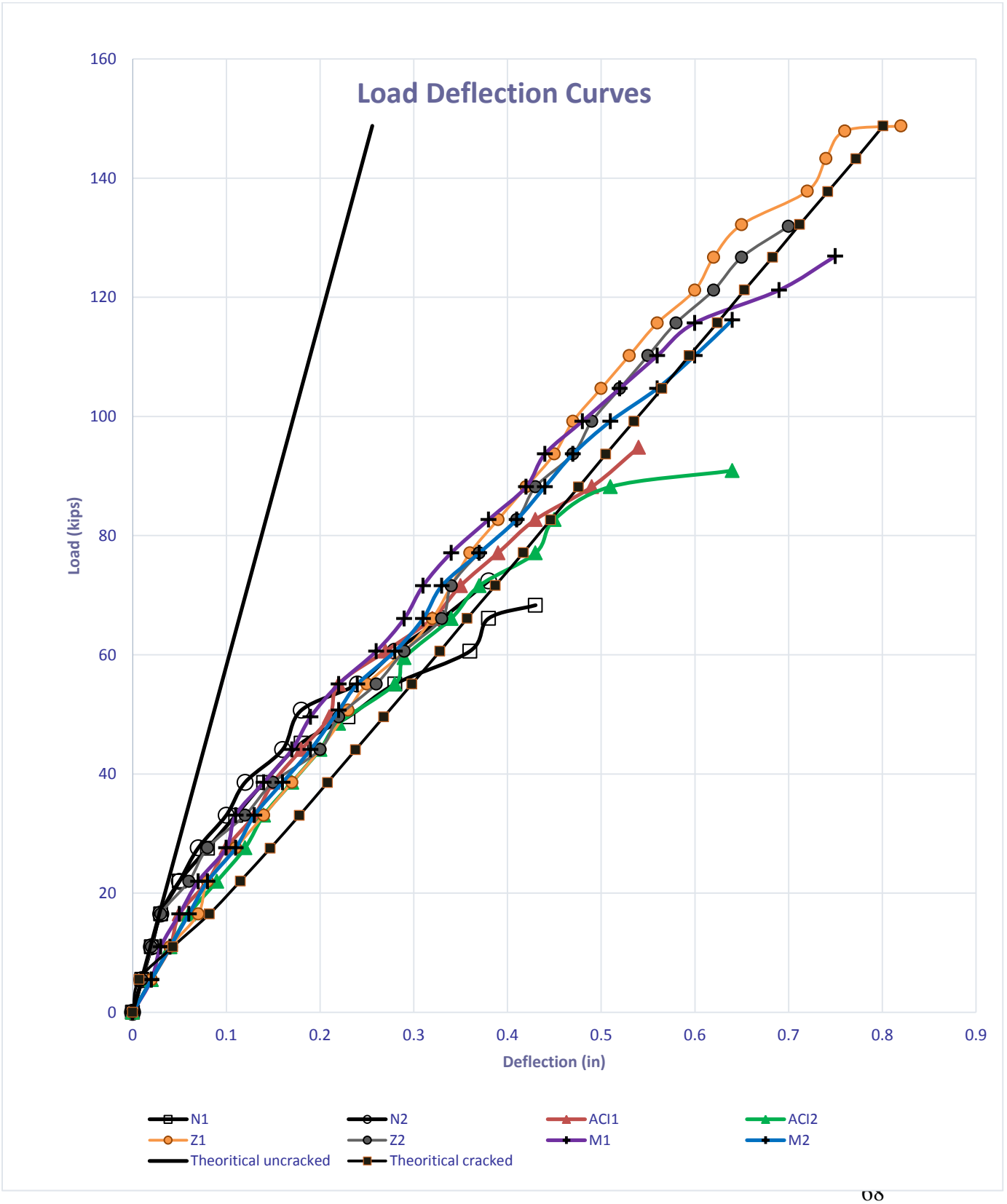

`

Fig 01: Average Load Deflection Response of Beams

`

Table 0-1 : Experimental an d theoretical values of " μ" for Modulus of Rupture

Beams	ρ_v	Experimental Cracking Moment (Kip-in)	Theoretical Cracking Moment (Kip-in)	Cracking Stress f_r		Value of μ	
				Experimental (psi)	Theoretical (psi)	Experimental	Theoretical
N1	0	352.64	344.72	492.35	481.29	7.67	7.50
N2	0	440.8	344.72	615.44	481.29	9.59	7.50
A1	0.001307	506.92	344.72	707.76	481.29	11.03	7.50
A2	0.001307	551	344.72	769.30	481.29	11.99	7.50
Z1	0.004416	551	344.72	769.30	481.29	11.99	7.50
Z2	0.004416	440.8	344.72	615.44	481.29	9.59	7.50
M1	0.003154	440.8	344.72	615.44	481.29	9.59	7.50
M2	0.003154	440.8	344.72	615.44	481.29	9.59	7.50

Table 0-2 : Shear Strengths of Specimens

Beam	Experimental Vexp (Kips)	ACI 318-11		Zararis Equation		Modified Equation	
		Vaci (Kips)	Vexp/Vaci	Vzar (Kips)	Vexp/Vzar	Vmod (Kips)	Vexp/Vmod
N1	34.16	20.53	1.664	28.35	1.205	28.37	1.204
N2	36.18	20.53	1.762	28.35	1.276	28.37	1.275
Avg,	**35.170**	**20.53**	**1.713**	28.35	**1.241**	28.37	**1.240**
A1	47.39	28.90	1.640	37.89	1.251	40.83	1.161
A2	45.46	28.90	1.573	37.89	1.200	40.83	1.113
Avg,	**46.422**	**28.90**	**1.606**	37.89	**1.225**	40.83	**1.137**
Z1	74.385	48.69	1.528	60.48	1.230	70.32	1.058
Z2	65.9547	48.69	1.355	60.48	1.091	70.32	0.938
Avg,	**70.170**	**48.69**	**1.441**	60.48	**1.160**	70.32	**0.998**
M1	63.37	40.65	1.559	51.30	1.235	58.33	1.086
M2	58.08	40.65	1.429	51.30	1.132	52.77	1.101
Avg,	**60.720**	40.65	**1.494**	51.30	**1.184**	52.77	**1.093**

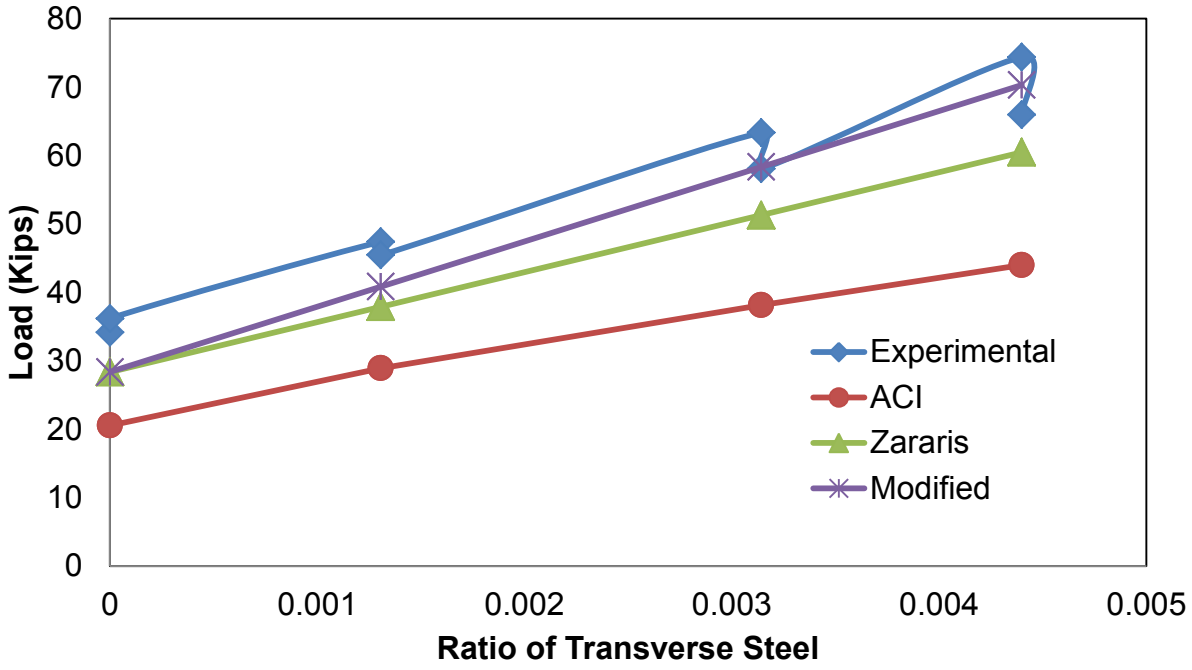

Figure 0-2 : Transverse Steel Ratio Vs Ultimate Shear Strengths Comparison of Specimens

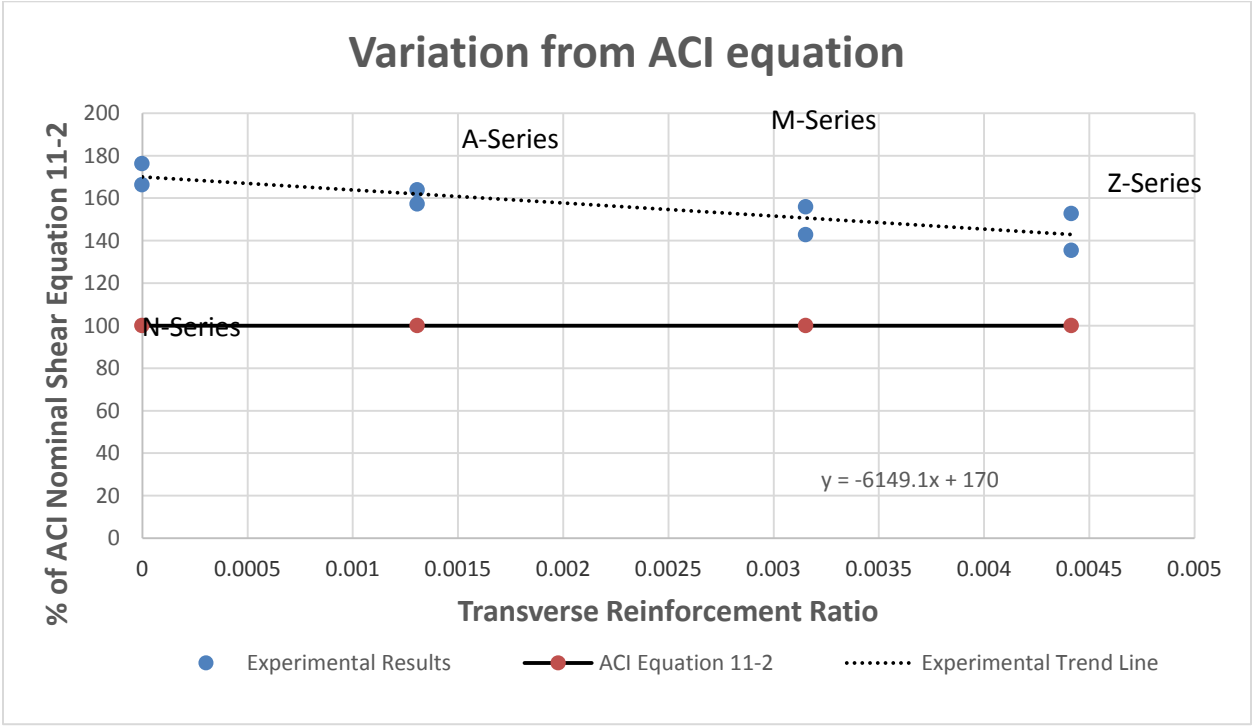

Figure 0-3: Variation in Experimental Shear Strength from ACI Theoretically calculated shear strengths

`

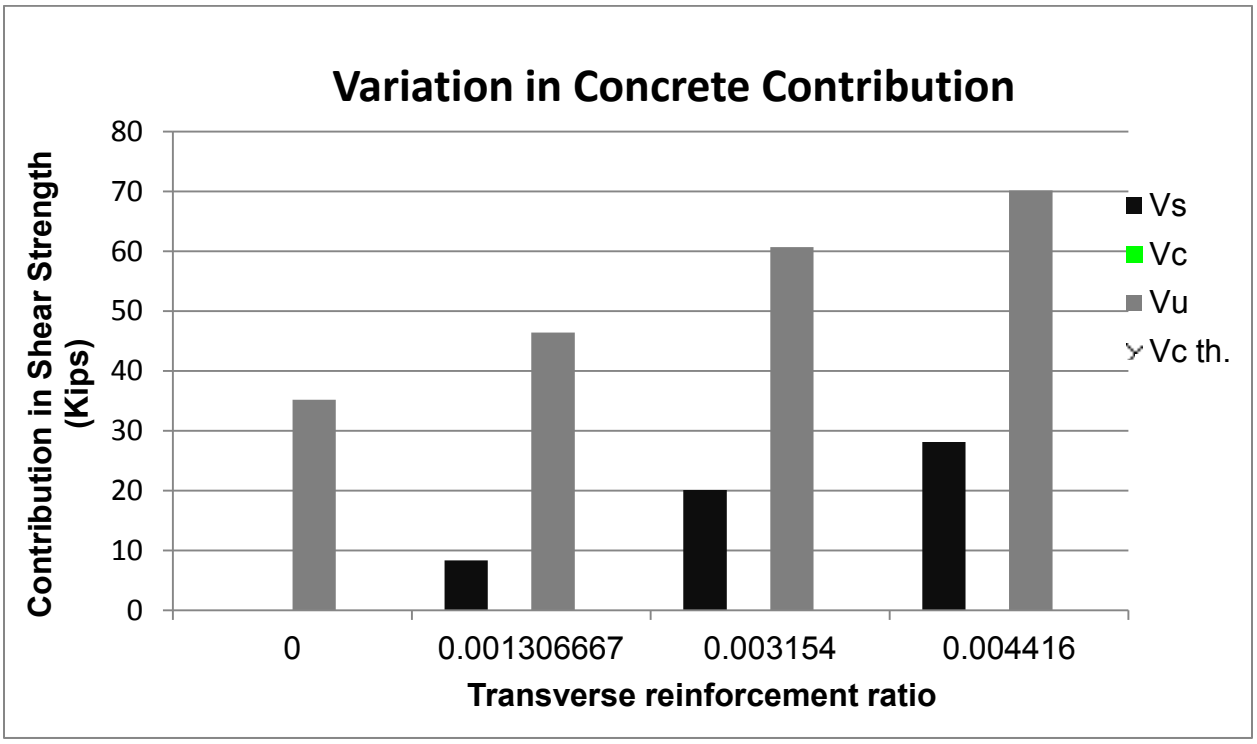

Figure 0-4 : Variation in Concrete Contribution from ACI Predicted Strengths

Table 0-3 : Experimental Values of γ for concrete shear strength

Beam	Experimental Strength (Kips)			ACI Predicted Strength (Kips)			Value of γ
	Vc	Vs	Vu	Vc	Vs	Vu	
N1	34.162	0	34.162	20.53	0	20.53	3.33
N2	36.17866	0	36.17866	20.53	0	20.53	3.52
Mean Value	**35.17**	**0**	**35.17**	**20.53**	**0**	**20.53**	**3.43**
A1	39.02	8.36	47.386	20.53	8.36	28.90	3.80
A2	37.09	8.36	45.4575	20.53	8.36	28.90	3.61
Mean Value	**38.06**	**8.36**	**46.42**	**20.53**	**8.36**	**28.90**	**3.71**
Z1	46.23	28.16	74.385	20.53	28.16	48.69	4.50
Z2	37.79	28.16	65.9547	20.53	28.16	48.69	3.68
Mean Value	**42.01**	**28.16**	**70.17**	**20.53**	**28.16**	**48.69**	**4.09**
M1	43.26	20.11	63.365	20.53	20.11	40.64	4.21
M2	37.97	20.11	58.0754	20.53	20.11	40.64	3.70
Mean Value	**40.61**	**20.11**	**60.72**	**20.53**	**20.11**	**40.64**	**3.96**

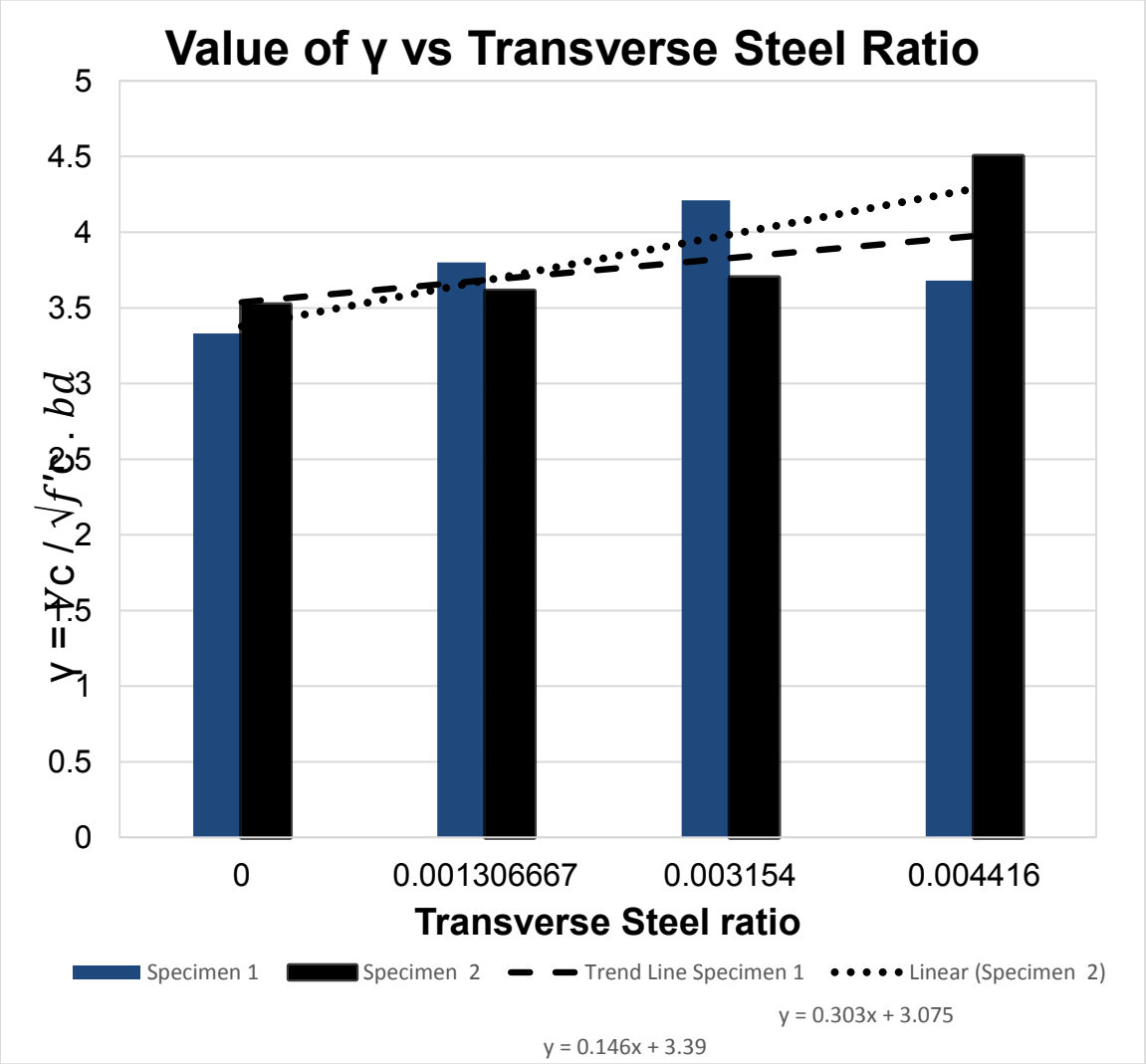

Figure 0-5 : Experimental Trend of γ for concrete shear Strength

`

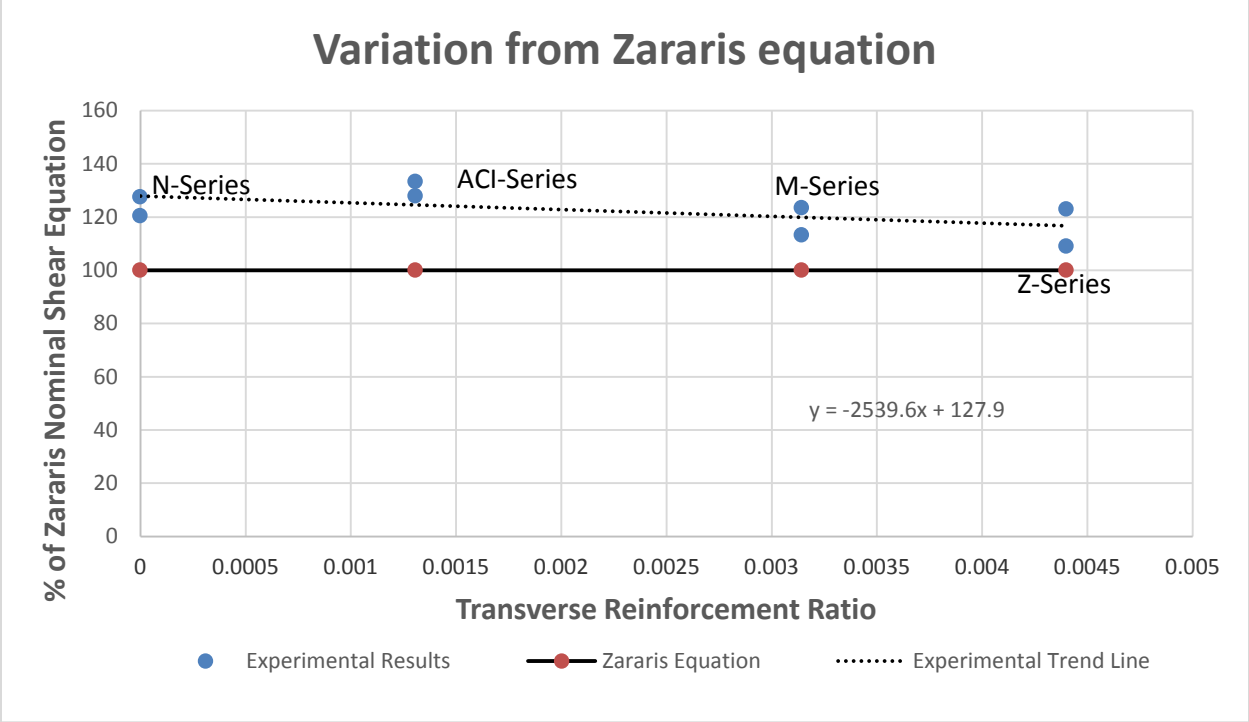

Figure 0-6 : Shear Strength Variation from Zarari's Equation

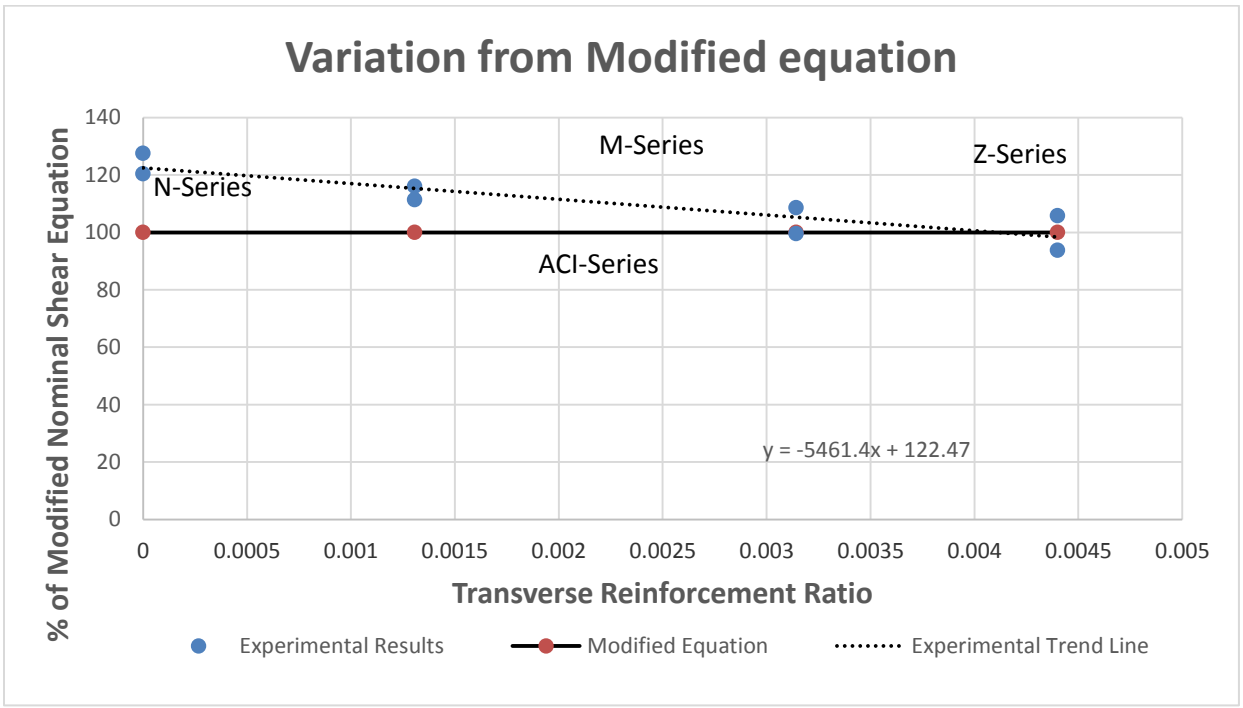

Figure 0-7 : Shear Strength Variation from Modified Zarari Equation.

`

Table 0-4 : Achieved Flexural Capacity of Beams

Beam	(Row)v	Mn Theoretical (K-ft)	P Ultimate (Kips)	M Experimental (K-ft)	% of Mn Theoretical
N1	0	219.99	68.32	113.8733	51.76
N2	0	219.99	72.36	120.5955	54.82
A1	0.001306667	219.99	94.77	157.9533	71.80
A2	0.001306667	219.99	90.92	151.5250	68.88
Z1	0.004416	219.99	148.77	247.9500	112.71
Z2	0.004416	219.99	131.90	219.8333	99.93
M1	0.003154	219.99	126.73	211.2167	96.01
M2	0.003154	219.99	116.15	193.5847	88.00

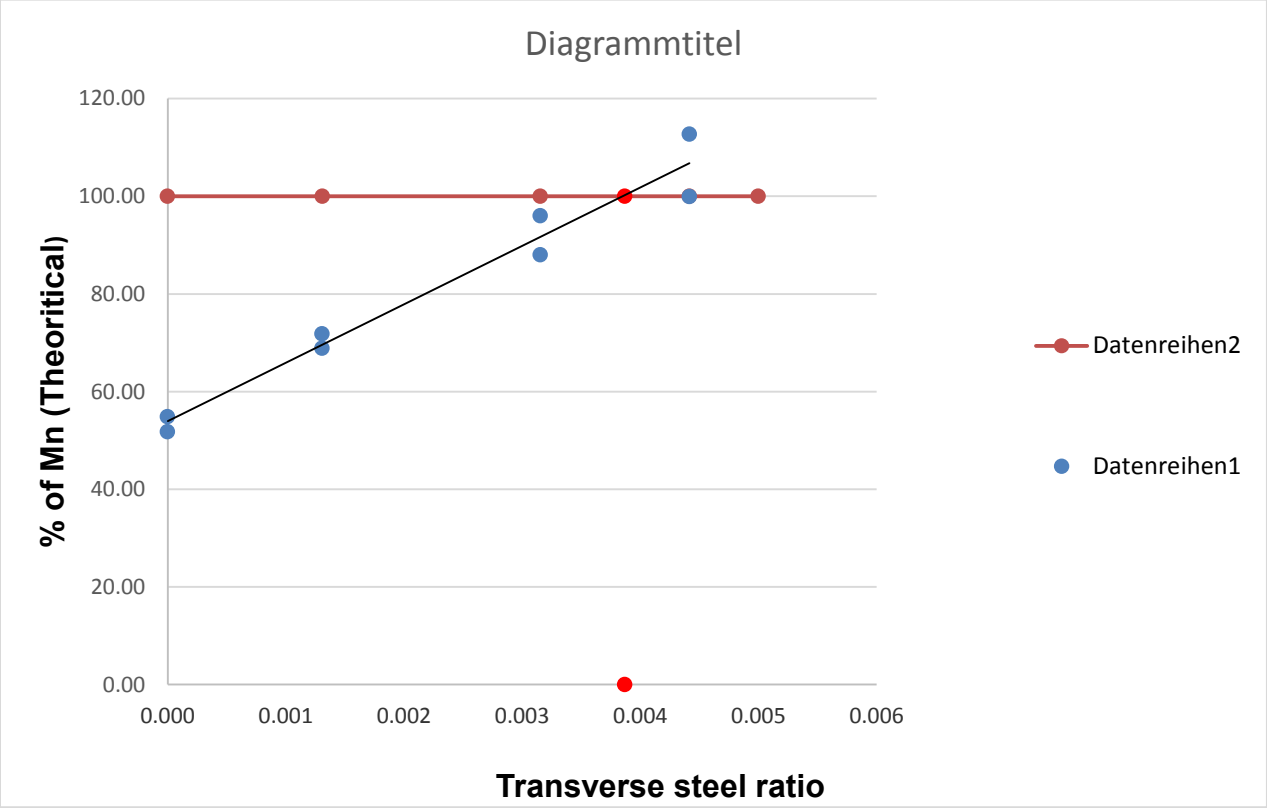

Figure 0-8: Transverse Steel Ratio vs Achieved Moment Capacity

`

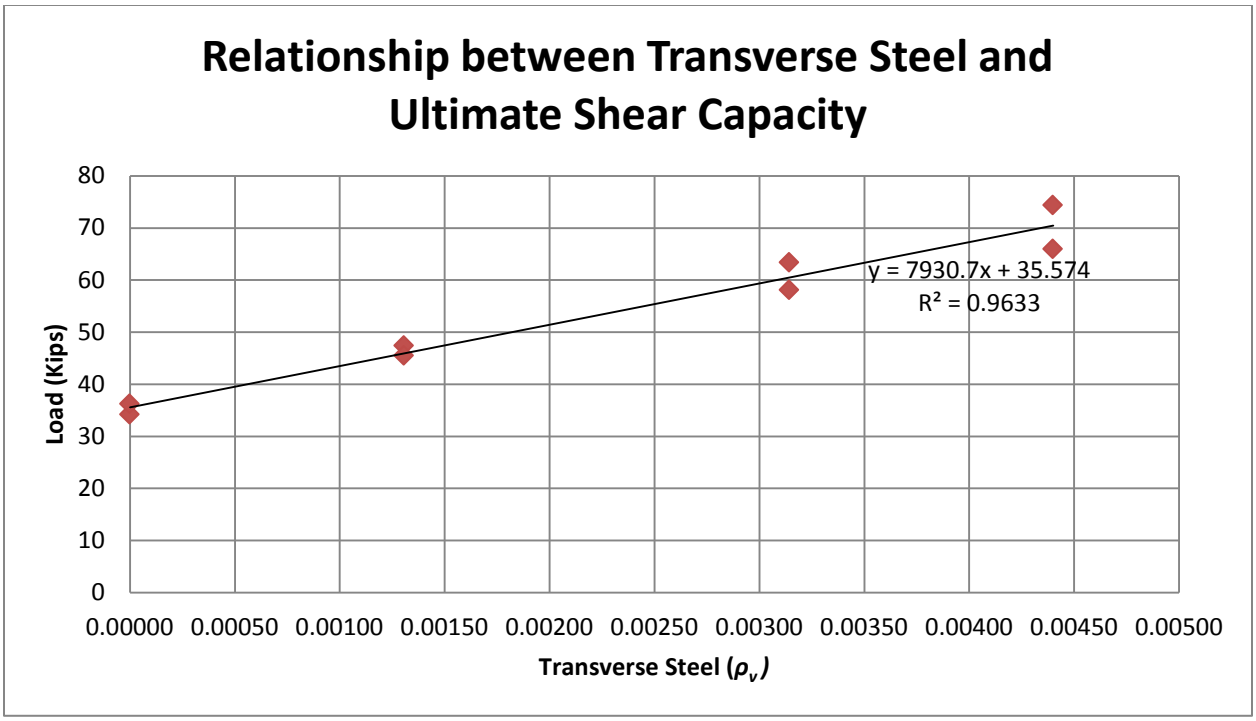

Figure 0-9 : Transverse Steel ratio Vs Achieved shear Strength

Development of Relationship between Minimum Shear Reinforcement and Flexural Capacity

Equating the experimentally obtained and the nominal moment capacities

$$V_u * a = A_s f_y (d - \frac{a}{2})$$

$$V_u = \frac{A_s f_y}{a} d(1 - \frac{a}{2d})$$

$$V_u = \frac{A_s f_y}{(a/d)} (1 - \frac{A_s f_y}{1.7 f'_c bd}) \qquad \therefore \ (a = \frac{A_s f_y}{0.85 f'_c b})$$

$$V_u = \frac{A_s f_y}{(a/d)} (1 - \frac{\rho f_y}{1.7 f'_c})$$

Ultimate shear capacity is a combination of shear strength provided by steel and concrete;

$$V_c + V_s = \frac{A_s f_y}{(a/d)} (1 - \frac{\rho f_y}{1.7 f'_c}) \qquad \therefore \ (V_u = V_c + V_s)$$

$$V_s = \left[\frac{A_s f_y}{(a/d)} (1 - \frac{\rho f_y}{1.7 f'_c}) - V_c \right]$$

Using ACI 318 Eqs. (11.3 and 11.15), V_s and V_c can be replaced as under;

$$\frac{A_v f_{yv} d}{s} = \left[\frac{A_s f_y}{(a/d)} (1 - \frac{\rho f_y}{1.7 f'_c}) - \gamma \sqrt{f'_c} bd \right]$$

$$\frac{A_v f_{yv}}{bs} = \left[\frac{A_s f_y}{bd(a/d)} (1 - \frac{\rho f_y}{1.7 f'_c}) - \gamma \sqrt{f'_c} \right] \qquad \text{(dividing by 'bd' on both sides)}$$

$$\rho_v f_{yv} = \left[\frac{\rho f_y}{(a/d)} (1 - \frac{\rho f_y}{1.7 f'_c}) - \gamma \sqrt{f'_c} \right]$$

Shear reinforcement ratio required for obtaining the nominal moment capacity can be expressed as;

$$\rho_v = \frac{1}{f_{yv}} \left[\frac{\rho f_y}{(a/d)} (1 - \frac{\rho f_y}{1.7 f'_c}) - \gamma \sqrt{f'_c} \right]$$

REFRENCES

[1] Mörsch, E., "Concrete-Steel Construction", McGraw-Hill, New York (English translation by E.P. Goodrich)

[2] Ritter, W. (1899). "Die Bauweise Hennebique " Schweizensche Bauzeitung, 33(7), 59-61.

[3] Jame. K. Weight and James G Macgregor (2005). Reinforced concrete members

[4] Kani, G. (1964). The Riddle of Shear Failure and Its Solutions. ACI Journal, 61 (4),441-467.

[5] Prodromos D. Zararis, "Shear Strength and Minimum Shear Reinforcement of Reinforced Concrete Slender Beams," ACI Structural Journal, V. 100, No. 2, March – April 2003, pp. 203 – 214.

[6] Collins, M., Bentz, E., Sherwood, E., & Xie, L. (2007). An adequate theory for the shear strength of reinforced concrete structures.

[7] Braestrup, M. (2009). Structural Concrete Beam Shear - Still a Riddle? ACI Special Publication, 265, 327-344.

[8] Collins, M. P., and Mitchell, D., "A Rational Approach to Shear Design-The 1984 Canadian Code Provisions." ACI Journal, Vol 83, No 6, 1986, pp. 925-933.

[9] Adebar, P., "Testing Structural Concrete Beam Elements", RILEM: Mat. And Struct, Vol 27, No 172, 1994, pp. 445-451.

[10] Leonhardt, F., & Walther, R. (1961-1962). Contribution to the treatment of shear in reinforced concrete (Vol. Technical Translation 1172). (J. Verschuren, & J. MacGregor, Trans.) National Research Council of Canada.

[11] Kani, G. (1967). How safe are our large reinforced concrete beams. ACI Journal 64 (3), 128-141

[12] Gupta, P., Collins, M.P., "Behavior of Reinforced Concrete Members Subjected to Shear and Compression", Report, Department of Civil Engineering, University of Toronto, Canada, 1993.

[13] Mattock, A.H., "Diagonal Tension Cracking in Concrete Beams with Axial Forces",

[14] Jung-Yoon Lee and Uk-Yeon Kim, "Effect of Longitudinal Tensile Reinforcement Ratio and Shear Span-Depth Ratio on Minimum Shear Reinforcement in Beams," ACI Structural Journal, V. 105, No. 2, March – April 2008, pp. 134 – 144.

[15] Taylor, H.P.J., "Investigation of the Forces Carried Across Cracks in Reinforced Concrete Beams in Shear by Interlock of Aggregate", Cement and Concrete Association, London, 1970, 22 pp.

[16] König, G, Grimm, R., Remmel, G., "Shear Behavior of Longitudinally Reinforced Concrete Members of HSC", Darmstadt Concrete, Vol. 8, 1993, pp. 27-42.

[17] Pendyala, R.S., Mendis, P., "Experimental Study on Shear Strength of High- Strength

Concrete Beams", ACI Structural Journal, Vol. 97, No4, 2000, pp. 564-571. Journal of Structural Division, ASCE, Vol. 95, September 1969, pp. 1887-1900.

[18] Reineck, K.-H., Kuchma, D., Kim, K.S., and Marx, S., "Shear Database for Reinforced Concrete Members without Shear Reinforcement", ACI Structural Journal, Vol 100, No 2, 2003, pp. 240-249.

[19] Ziara, M. M. (1993). The influence of confining the compression zone in the design of structural concrete beams. Heriot-Watt University.

[20] Jansen and A. Lapko, "On Shear Reinforcement Design of Structural Concrete Beams On the Basis of Theory of Plasticity," Journal of Civil Engineering and Management, V. 15, No. 4, 2009, pp. 395 – 403.

[21] Alexander Placas and Paul E. Regan, "Shear Failure of Reinforced Concrete Beams," ACI Journal, 1971, pp. 763 – 773.

[22] Evan C. Bentz, Frank J. Vecchio and Michael P. Collins, "Simplified Modified Compression Field Theory for Calculating Shear Strength of Reinforced Concrete Elements," ACI Structural Journal, V. 103, No. 4, July –August 2006, pp. 614 – 624.

[23] Aurelio Muttoni and Miguel F. Ruiz, "Shear Strength of Members without Transverse Reinforcement as Function of Critical Shear Crack Width," ACI Structural Journal, V. 105, No. 2, March – April 2008, pp. 163 – 172.